



13th EUROPEAN CONFERENCE ON PRECISION AGRICULTURE – HUNGARY

Budapest, 19-22. July 2021

BOOK OF ABSTRACTS OF ALL THE POSTERS



Hosted by:



Supported by:



In cooperation with:



The 2021 ECPA was sponsored by the following organisations

Golden cooperation partners:



Silver cooperation partners:



Bronze cooperation partner:

Tomelilla Kft.

Online exhibitor:



Cooperation partners:



Published by Magyarországi Precíziós Gazdálkodási Egyesület
ISBN 978-615-01-2017-1

To cite these proceedings please use:

Author(s) (2021). Poster Title. In: J. V. Stafford - G. Milics (eds.): Poster Proceedings of the 13th European Conference on Precision Agriculture, July 19-22, Budapest, Hungary,. pp.XX. Magyarországi Precíziós Gazdálkodási Egyesület. ISBN 978-615-01-2017-1

FOREWORD

Dr. Gabor Milics, PhD, Conference Chair

July 03, 2021, Hungarian Society of Precision Agriculture, Budapest, Hungary

Dear Reader,

In 2017, at the 11th European Conference on Precision Agriculture (Edinburgh), the ECPA conference organizing committee decided that the right of organizing the next conferences will be 2019 SupAgro (Montpellier, France) and 2021 Hungarian Society of Precision Agriculture (Budapest Hungary).

Without being superstitious, the number “13” did not look good! However, at that time, we never thought about what difficulties would face us in the form of a pandemic by 2021. We had to make very difficult decision on risking the organization in the middle of lockdown, postponing the conference or going to on-line. None of the solutions would be acceptable individually, so we decided to have a hybrid event: the first ECPA organized with the possibility to attend in person or join the conference on-line.

The organizers met challenges in every aspect of the preparatory work. However, in spite of all the uncertainties, we sincerely hope that the 13th European Conference on Precision Agriculture will result in a profitable meeting – attending in-person, or on-line – for everyone and will provide new information and solutions for the challenges that agricultural practice is facing.

We are grateful to the International Society of Precision Agriculture (ISPA) for support in communicating the conference news to the members of the Society. The Hungarian Society of Precision Agriculture and the Organizing team would especially like to thank and congratulate Dr. John V. Stafford, the editor of the proceedings, for the enormous work he has done for the conference during the last couple of months sometimes with very tight schedule and very close deadlines. In addition, the organizers would like to thank all members of the conference Scientific Committee: for the International Committee for their invaluable contribution in supporting the editor and assuring the scientific quality of the communications presented at this conference and the Local Scientific Committee for the help in organizing the program.

We appreciate the financial contribution of all the sponsors of the 13th ECPA conference, and would like to highlight the support from the Ministry of Agriculture, Hungary and would like to especially thank Dr. István Nagy, Minister for Agriculture, Hungary for being the patron of the conference. We would like to express our gratitude to all the authors – without whom there would be no conference - and attendees. At the time of writing this foreword (early July 2021), we already know the poster session can only be organized in the on-line space of the 13th ECPA conference. In spite of the fact that poster presenters will be attending on-line, we hope they will follow the conference and prepare their papers for the next conference, when we can all meet in person!

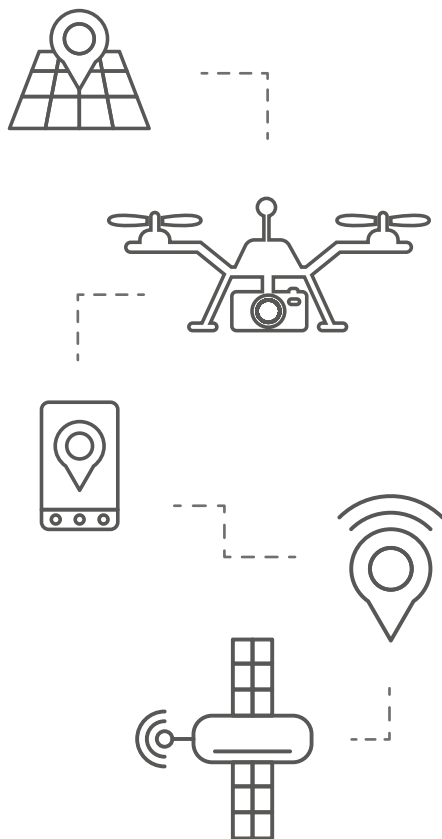
Finally, as Chair I am grateful to all the conference Organizing Committee for their support, and hard work over the past two years – some have been involved in the process for even longer time – in bidding for and delivering this conference. Preparation for the technical tour takes a long time and requires extra effort from the host farm – KEVE Zrt. – and the cooperating partners, making possible to show PA practices in Hungary. Very special thanks go to the technical tour organizing team! Generally, without the great conference and technical tour organizing team - I had the chance to work with - it would be impossible to do this fantastic work!

We – The 13th ECPA Organizing Committee – are both honoured and delighted to have worked for you and to have helped in showing “Adoption of innovative precision agriculture technologies and solutions” series of ECPA conferences.

Have a great Conference!

Sikeres konferenciát!

Gabor



More information: www.ecpa2021.hu

ESTIMATION OF THE IMPORTANCE OF BIOTIC AND ABIOTIC VARIABLES FOR THE DETECTION OF CERCOSPORA - LEAF SPOT DISEASE BASED ON OPTICAL SENSORS	8
Ispizua Yamati F. R., Barreto A. Bömer J., Streit S., Paulus S., Mahlein A-K.	
IDENTIFYING AFLATOXIN CONTAMINATION RISK ZONES WITHIN FIELDS FOR PRECISION MANAGEMENT	10
R. Kerry ¹ , B. Ingram ² , B. Ortiz ³ , D. Damianidis ³ , H. Stone ³	
SPECTRAL ASSESSMENT OF CHICKPEA MORPHO-PHYSIOLOGICAL TRAITS FROM SPACE, AIR AND GROUND	12
Sadeh R. ¹ , Avneri A. ¹ , Tubul Y. ¹ , Lati N. R. ² , Abbo S. ¹ , Bonfil J. D. ³ , Peleg S. ¹ , Herrmann I. ¹	
EVALUATION OF DIFFERENT VOLUME ESTIMATION APPROACHES FROM MULTI-TEMPORAL LIDAR DATA IN STRAWBERRY	13
K.K. Saha, N. Tsoulas, M. Zude-Sasse	
AN APPROACH TO SEGMENT WOOD STRUCTURE USING LIDAR SCANNER IN APPLE TREES	15
N. Tsoulas, M. Penzel, M. Zude-Sasse	
AN APPROACH FOR THE USE OF RGB-DEPTH PERCEPTION FOR PRUNING VINEYARD ESTIMATION	17
Rueda-Ayala V. ¹ , Moreno H. ² , Ribeiro A. ² , Andujar D. ²	
ESTIMATING OCCLUDED GRAPE BUNCHES USING IMAGE ANALYSIS – CASE STUDY WITH CV. ‘ARINTO’	19
G. Victorino ^{1,2} , R. Braga ¹ , J. Santos-Victor ² , C. M. Lopes ¹	
HYPERSPECTRAL IMAGING AND MACHINE LEARNING FOR PEST AND DISEASE DETECTION IN COMMERCIAL VINEYARDS	21
Hernández I. ¹ , Gutiérrez S. ² , Alonso M. ¹ , Ceballos S. ¹ , Iñiguez R. ¹ , Palacios F. ¹ , Diez-Navajas A. M. ³ , Tardaguila J. ¹	
IN-FIELD DOWNY MILDEW DETECTION IN GRAPEVINE USING COMPUTER VISION AND CONVOLUTIONAL NEURAL NETWORKS	23
Hernández I. ¹ , Gutiérrez S. ² , Ceballos S. ¹ , Iñiguez R. ¹ , Palacios F. ¹ , Diez-Navajas A. M. ³ , Tardaguila J.	
EVALUATING THE POTENTIAL OF POTATO YIELD MAPPING USING HIGH SPATIAL AND TEMPORAL RESOLUTION PLANETSCOPE SATELLITE IMAGES	25
Mizuta K. ¹ , Miao Y. ¹ , Lacerda L.N. ¹ , Rosen C. ¹ , Gupta S. ¹ , Kang S.K. ¹ , Huang Y. ²	
OBTAINING REMOTE SENSOR DATA OF FRUIT TREES BY MEANS OF CIRCULAR CONVEYOR SYSTEM	27
Zude-Sasse M., Tsoulas N., Elwert S., Geyer M.	

BIOMASS ESTIMATIONS OF PERENNIAL RYEGRASS USING UAV-BASED MULTISPECTRAL BANDS AND VEGETATION INDICES	29
Pranga J. ^{1,2} , Borra-Serrano I. ¹ , De Swaef T. ¹ , Aper J. ¹ , Ghesquiere A. ¹ , Roldán-Ruiz I. ^{1,3} , Janssens I. ² , Ruyschaert G. ¹ , Lootens P. ¹	
COMBINED TRAFFIC CONTROL OF IRRIGATION ON HETEROGENEOUS FIELD	31
A. Nagy ¹ , A. Szabó ¹ , Cs. Juhász ¹ , B. Gálya Farkasné ¹ , Á. Kövesdi ² and J. Tamás ¹	
TOWARDS A SATELLITE-BASED DELINEATION AT THE TERRITORIAL SCALE IN HIGH YIELDING ENVIRONMENT TO SUPPORT THE MANAGEMENT OF NITROGEN	33
Lenoir A. ¹ , Dumont B. ¹ & Vandoorne B. ¹	
WHY THE EVALUATION OF SPATIALIZED CROP MODELS NEEDS TO DIFFER FROM CURRENT APPROACHES TO MODEL EVALUATION?	35
Pasquel D. ¹ , Cammarano D. ² , Richetti J. ³ , Roux S. ⁴ , Tisseyre B. ¹ , Taylor J.A. ¹	
AGRO IOT PLATFORMS AND SENSORS IN CROP PRODUCTION	37
Ambrus B., Nyéki A., Teschner G., Neményi M., Milics G., Kovács A. J.	
DEVELOPMENT OF A LOW-COST PORTABLE PAR DEVICE FOR CROP MANAGEMENT	39
Coffin A. ¹ , Bonnefoy-Claudet C. ² , Jansen A. ² and Chassigne M. ² , Gée C.	
OPPORTUNITIES FOR MORE PRECISE WEED MANAGEMENT IN FIELDS OF LOWLAND RICE IN SOUTH-EASTERN NIGERIA.	41
Ukwoma-Eke, O., Murdoch, A. J.	
ENCOURAGING TECHNOLOGY TAKE-OFF WITH FARMER CHAMPIONS AND STUDENT AMBASSADORS	43
G. Rose ¹ , A.J. Murdoch ¹ , D.S. Paraforos ² , T. Pavlenko ² , J. Draper ³ , L.M. Battaglini ⁴ , P. Cornale ⁴ , M. Renna ⁵ , N. Scollan ⁶ , I. Marshall ⁶ , R. Negrini ⁷ , M. Favoro ⁷ and I. Pascarella ⁷	
NUDGING ARABLE FARMERS TOWARDS GREATER ADOPTION OF PRECISION AGRICULTURE	45
Antognelli, S. ¹ , Murdoch, A. ² , Guidotti, D. ¹ , Ranieri, E. ¹ , Ahrholz, T. ³ , Tranter, R. ² , Engel, T. ³ , Mahmood, S. ² , Paraforos, D.S. ⁴ , Todman, L. ²	

ESTIMATION OF THE IMPORTANCE OF BIOTIC AND ABIOTIC VARIABLES FOR THE DETECTION OF CERCOSPORA - LEAF SPOT DISEASE BASED ON OPTICAL SENSORS

Ispizua Yamati F. R., Barreto A. Bömer J., Streit S., Paulus S., Mahlein A-K.
Institute of Sugar Beet Research (IfZ), Göttingen, Germany

Sugar beet is the only crop that produces high-quality sugar under a temperate climate, making it the essential sugar source in Europe. Plant diseases are one main limitation to yield development. In sugar beet, one of the most destructive foliar diseases is Cercospora Leaf spot (CLS) disease caused by *Cercospora beticola* Sacc. Early and accurate detection is essential to avoid yield losses and evaluate the necessity of a fungicide application.

Interaction between plant and pathogen and symptom development leads to changes in the reflection properties of above-ground plant organs. The combination of optical sensors with machine learning techniques has shown high capabilities to improve the detection and monitoring of plant disease in crop production. However, weather conditions and environmental factors and their interaction strongly impact disease spreading and development. For CLS, the main spreading occurs through conidiospores, primarily by wind and splashing water (Lawrence, 1970). The conidia production is also affected by two main parameters, temperature and relative humidity (Bleiholder & Weltzien, 1971; Bleiholder & Weltzien, 1972). The aforementioned factors combined with the morphological characteristics of the plant need to be considered to approach an early and accurate detection of diseases. This work aims to determine which of the biotic and environmental factors are of great importance in predicting disease severity and making technological progress in predicting and monitoring CLS in sugar beet fields.

In 2020, a field trial was conducted near Göttingen, Germany, to investigate the pathogen's spread and its interaction with the environment. Immediately after sowing, some experimental field areas were inoculated with *C. beticola* to simulate an infection. Georeferenced IoT microclimate sensors were installed to quantify temperature and humidity around the field. After that, growing degree days (GDD, base temperature = 1.1 °C) and the number of possible generations (Bleiholder & Weltzien, 1971) were calculated. In addition, multispectral images (blue, green, red, red edge, and near-infrared and long-wave infrared) were taken weekly from sowing to harvest with a multispectral camera mounted on an unmanned aerial vehicle. At the same time, a visual assessment of the respective disease severity (DS) was carried out to serve as reference data.

After preprocessing multispectral images, different values derived from the digital elevation model have been calculated, such as plant height, aspect, slope, watersheds and drainage basins, surface roughness, and the topographic convergence index. Additionally, several vegetation indices were calculated. The optimized soil adjusted vegetation index (OSAVI) presented the highest correlation with DS. Variables with low variance have been removed before being introduced into the model.

A gradient boosting algorithm was implemented to determine which are the most critical variables, and a SHAP (Shapley additive explanations, Liu et al 2020) for the ten most important variables were generated to facilitate interpretation.

As shown in Figure 1, the variable that contributes most to the detection was the OSAVI, the lower the index values, the higher the importance. In contrast, in the second place, are the GDD that the more advanced it is, the more influence the model has. In the third and fourth place are the red spectral band and plant height, respectively. The lower they are, the more effect and variation on the DS they have.

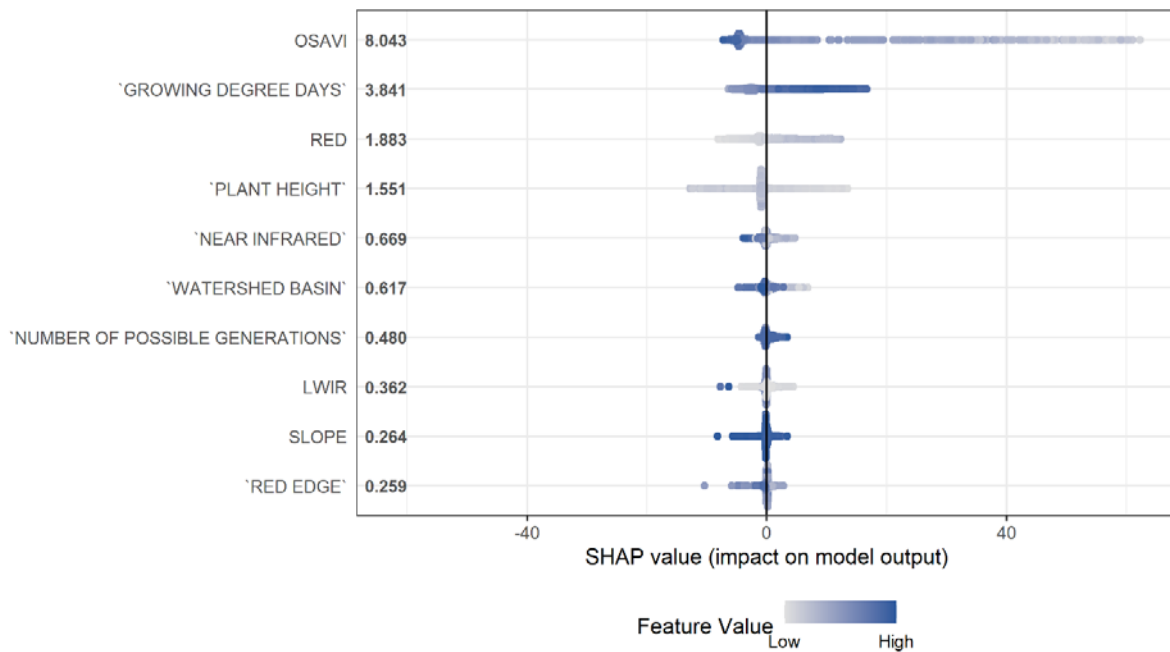


Figure 1: SHAP summary plot of the ten most important features for the gradient boosting algorithm for every sample, showing the impact of each feature on the model output. The y-axis indicates the variable in order of importance. OSAVI= Optimized soil adjusted vegetation index, LWIR= Long-wave Infrared, RED= Red band (668 nm center, 14 nm bandwidth), RED EDGE= Red edge band (717 nm center, 12 nm bandwidth).

The study successfully achieved the integration of sensor data with environmental data. The findings underline the importance of considering biotic and environmental factors to understand better the plant's response to disease infection. Furthermore, they highlight the need for measuring the heterogeneity of additional experimental parameters like soil, climate and cultivar.

Research results as provided by this study allow us to advance in the early detection of diseases. In addition, they enable reduction of computation time of models by discarding variables that are highly correlated with each other or that contribute poorly to the models' accuracy.

Bleiholder, H.; Weltzien, H. C. 1971: Beiträge zur Epidemiologie von *Cercospora beticola* Sacc. (Contributions to the epidemiology of *Cercospora beticola* Sacc.) in Zuckerrübe. In: Journal of Phytopathology 72 (4), S. 344–353. DOI: 10.1111/j.1439-0434.1971.tb03207.x.

Bleiholder, H.; Weltzien, H. C. (1972): Beiträge zur Epidemiologie von *Cercospora beticola* Sacc. (Contributions to the epidemiology of *Cercospora beticola* Sacc.) in Zuckerrübe. In: Journal of Phytopathology 73 (1), S. 46–68. DOI: 10.1111/j.1439-0434.1972.tb02524.x.

Lawrence, J. S. 1970: Wind dispersal of conidia of *Cercospora beticola*. In: Phytopathology 60 (7), S. 1076. DOI: 10.1094/Phyto-60-1076.

Liu, Y., Just, A. 2020. SHAPforxgboost: SHAP Plots for 'XGBoost.' R package version 0.1.0.

IDENTIFYING AFLATOXIN CONTAMINATION RISK ZONES WITHIN FIELDS FOR PRECISION MANAGEMENT

R. Kerry¹, B. Ingram², B. Ortiz³, D. Damianidis³, H. Stone³

¹Brigham Young University, UT, USA, ²Universidad de Talca, Curico, Chile, ³Auburn University, AL, USA

ruth_kerry@byu.edu

Background: Aflatoxin is a mycotoxin produced by *Aspergillus* fungi which can contaminate corn. It can cause liver cancer so there are legislative limits on the levels allowed in grain. Levels are measured at harvest and the whole crop accepted or rejected based on the average concentration. Reducing the amount of the crop rejected during high-risk years could be achieved by identifying zones within fields with different contamination risk. Zones could have differential planting and irrigation rates to reduce risk and could be harvested and stored separately to avoid rejection of the whole crop.

Contamination is primarily driven by high temperatures and drought conditions, during the mid-silk growth stage (June). Greater contamination risk within fields is likely in areas with light-textured soil, shedding topographic positions and aspects with greatest evapo-transpiration. As these are relatively permanent features of fields, the patterns of contamination risk are likely to be stable in time. Determining aflatoxin contamination levels of grain samples is expensive. Field observations were made in one high risk season (2010) and free remotely sensed (2006-2011), elevation and soil survey data were used to determine risks zones and if they were likely to be stable in time.

Methods: Total Aflatoxin concentrations (ppb) were measured in two non-irrigated corn fields in Southeast Alabama, USA. Each 13 ha field was divided into zones based on soil type and elevation and two locations within each zone were assessed for Aflatoxin with three replicates measured at each location. Minimum, maximum and mean Aflatoxin values on a 30 m grid were kriged from these values. Top- (0-30 cm) and sub-soil (40-100 cm) volumetric water content (VWC) and leaf chlorophyll (SPAD) were measured and kriged to a 30 m grid. Soil type was extracted from a soil survey map. Elevation data (30 m) was used to calculate modified catchment area (MCA) (Figure 1). LandSat 5 NDVI (30 m pixels) and thermal IR data from all cloud-free dates in the 2006 to 2011 growing seasons were extracted. The drought risk associated with each month and year was determined relative to 30 year normal average maximum monthly temperatures and precipitation totals for the nearest weather station.

Correlations between field and sensed data were examined. Best Subset regression was done with min., mean and max. Aflatoxin as dependent variables and June/July 2010 imagery, soil survey, elevation and field data as potential independent variables. Log NDVI and thermal IR data were used for bivariate local Moran's I (B_LMI) analysis. Imagery data were classified into two zones by K-means and the % agreement between classifications based on Aflatoxin values and imagery was determined.

Results: There were obvious correlations between Aflatoxin and elevation, topsoil VWC, MCA and these are strongest for min. and mean Aflatoxin (Figure 1). Thermal data was more strongly correlated with Aflatoxin than NDVI. The imagery data with largest correlations to Aflatoxin occurred when there was drought early in the growing season. The R² value for regression with max. Aflatoxin was larger than min. and mean Aflatoxin. Regression suggested that soil type was important for predicting Aflatoxin.

B_LMI analysis showed a significant cluster with low NDVI and high Thermal values each year (2006-2011) which corresponded to two soil series with the highest Aflatoxin values and formed the high-risk class (Figure 1 i).

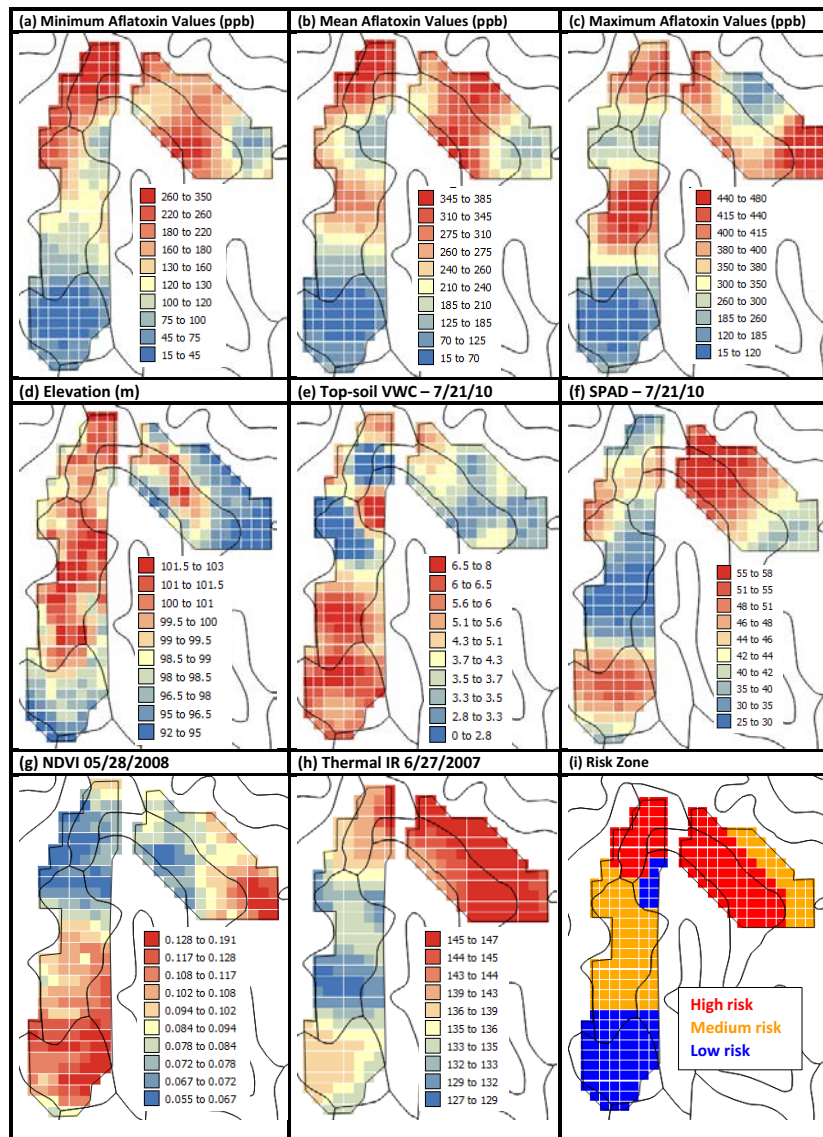


Figure 1: Pixel maps (30m) of (a) minimum, (b) mean, (c) maximum kriged aflatoxin, (d) elevation, (e) Top-soil VWC for 7/21/10, (f) crop SPAD measurements for 7/21/10, (g) NDVI 05/28/2008, (h) Thermal IR 6/27/2007 and (i) risk zones. Black line=soil type

The three regression plots showed two distinct groups of points which identified the low-risk zone (Figure 1 i). Comparison tests showed expected significant differences in Aflatoxin, top-soil VWC and 75% of imagery data between these three risk zones. Two class K-means classifications of imagery (2006-2011) showed 27-83% agreement for min., 42-86% for mean and 44-79% for max. Aflatoxin values. Classifications from imagery in months with the most droughty weather conditions showed the highest percentage agreements with Aflatoxin classifications.

Conclusions: The consistent spatial patterns in imagery over time (2006-2011) and associated with drought suggest the stability of Aflatoxin risk zones in time. This work suggested that elevation and soil type may be sufficient to define zones in other fields. For 2010 (a high-risk year), only the low-risk zone had values below the 100 ppb FDA aflatoxin limit and most of that zone exceeded the FDA 20 ppb limit. This suggests that irrigation or planting of resistant varieties should be practiced in this field.

SPECTRAL ASSESSMENT OF CHICKPEA MORPHO-PHYSIOLOGICAL TRAITS FROM SPACE, AIR AND GROUND

Sadeh R.¹, Avneri A.¹, Tubul Y.¹, Lati N. R.², Abbo S.¹, Bonfil J. D.³, Peleg Z.¹, Herrmann I.¹

¹*The Robert H. Smith Institute of Plant Sciences and Genetics in Agriculture, Faculty of Agriculture, Food and Environment, The Hebrew University of Jerusalem, Rehovot, Israel,*

²*Agricultural Research Organization (ARO), Newe Ya'ar Research Center, Israel,*

³*Agricultural Research Organization (ARO), Gilat Research Center, Israel*

Chickpea (*Cicer arietinum*) is an important grain legume in semi-arid regions and water-stress is a major constraint to its productivity. Area under chickpea cultivation is growing but climate change toward greater aridity results in higher precipitation instability and risks yields. The ability to assess water potential can support irrigation decisions. Thus, improved ability to spatially assess plants water status can promote more efficient irrigation. The current study aims to assess plant water status, leaf area index and grain yield by spaceborne, airborne and ground spectral sensors. Field experiments were conducted in two locations, representing different climatic conditions in Israel. Five irrigation regimes were applied: 50%, 75%, 100%, 120% and 140% of Penman-Monteith evapotranspiration were implemented at the Gilat research station and in a commercial field (Kibbutz Or-HaNer). Plants were characterized weekly for morpho-physiological traits and grain yield data was obtained at the final harvest. Canopy reflectance was acquired with a MicroSatellite VEN μ S (11 spectral bands, 420-910 nm), a drone mounted Rededge MicaSense camera (5 spectral bands, 470-860 nm; only in Gilat) as well as field spectrometer dual-field of view system at ground level (ASD, 350-2500 nm). The multispectral images as well as hyperspectral data were pre-processed to the level of reflectance. The VEN μ S and ground level hyperspectral data were divided to calibration and validation data sets while the multispectral 5 bands imagery was analyzed only for calibration data set. Morpho-physiological traits and grain yield values were showing differences between most of the irrigation regimes. The spectral data acquired from spaceborne, airborne and ground sensors were capturing the variability in canopy reflected resulted from the irrigation regimes. The VEN μ S, 5 bands airborne imagery and hyperspectral ground level data are useful for distinguishing chickpea plant status and evaluation of morpho-physiological traits.

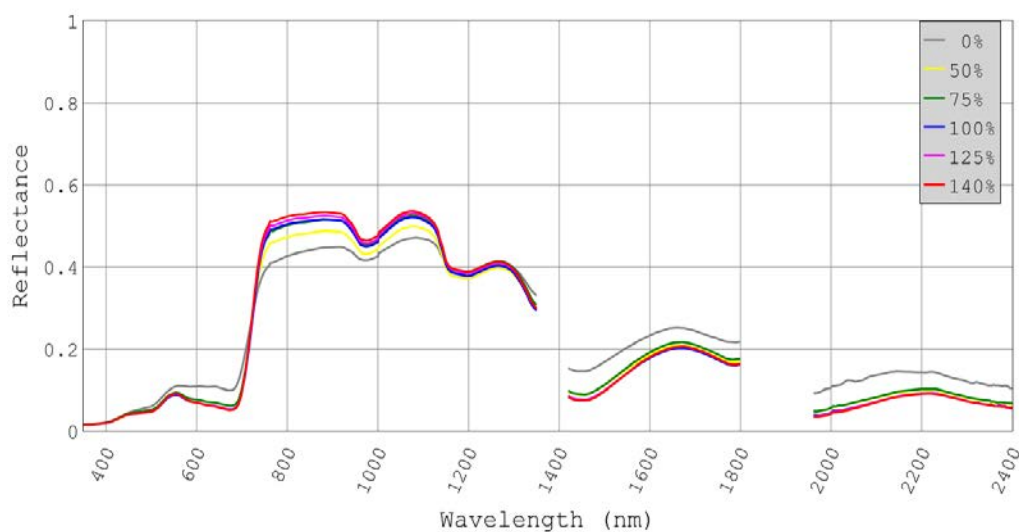


Figure 1: Canopy ground level hyperspectral reflectance in Gilat of the irrigation regimes, 95 days after emergence (21 days after implementation of irrigation regimes)

EVALUATION OF DIFFERENT VOLUME ESTIMATION APPROACHES FROM MULTI-TEMPORAL LIDAR DATA IN STRAWBERRY

K.K. Saha, N. Tsoulias, M. Zude-Sasse

Leibniz Institute for Agricultural Engineering and Bioeconomy (ATB), Dept. Horticultural Engineering, Potsdam, Germany

Email: ksaha@atb-potsdam.de

INTRODUCTION

Estimation of plant canopy volume is an important task for horticultural crop growers who aim to adapt the concept of precision agriculture to the production processes in fruit production. Plant volume information supports growers in two ways, i) it helps to understand the growth dynamics and ii) it provides the basis for calculating precisely the amount of inputs e.g., fertilizer application, plant protection and thinning spraying, irrigation etc. that can be applied at variable rate adjusted to each individual fruit tree. Technological development of mainly optical sensors can assist to obtain precise plant information remotely. Particularly light detection and ranging (LiDAR) sensors can provide three-dimensional (3D) plant information as point cloud (Tsoulias et al. 2020). In recent years, LiDAR has been employed by agricultural researchers in horticulture (Underwood et al. 2016) and forestry researchers (Yan et al. 2019) for the estimation of tree canopy volume. Most of the approaches that have been reported referred to tree crops but a few limited research works have been found on small horticultural plants, for example strawberry (*Fragaria × ananassa*) which is a perennial herb plant. In this study, a comparative assessment was carried out for different volume estimation approaches utilizing temporal strawberry point cloud data acquired with a linear conveyor mounted LiDAR scanner.

MATERIALS AND METHODS

For this study, strawberry (*Fragaria × ananassa*) plants (n=4) of a commercial cultivar ‘Honeoye’ were planted at 2-3 leaves stage (BBCH 13) in the experimental station of Leibniz Institute for Agricultural Engineering and Bio-economy (ATB) located in Marquardt, Germany. Each strawberry plant was planted in separate containers, while a 2D LiDAR laser scanner (LMS511 pro model, Sick, Germany) was used to scan the plants. The LiDAR was mounted on a movable linear conveyor system (Module 115/42, IEF Werner, Germany) with maximum length of 800 mm. The conveyor system was operated by a servo positioning controller (LV-servoTEC S2, IEF Werner, Germany) and S2 Commander software (version 4.1.4201.1.1, IEF Werner, Germany). The linear conveyor system consisted of a tooth-belt carrier which can run vibration free at variable speed with ± 0.05 mm accuracy. The LiDAR measurement and reference data collection were carried out in 2-3 week interval for 12 weeks. LiDAR scanning was performed from two opposite sides at 1 m distance between sensor and plant center. 3D point clouds of two opposite sides of each plant were processed using own Python code. The outliers were filtered using a sparse outlier removal technique. Both point clouds were aligned and merged to get the strawberry plant point clouds. Reference data captured plant canopy volume, measuring width and height of the plants and considering cylindrical shape. For estimation of canopy volume from a 3D point cloud, three approaches were implemented: (i) convex hull, (ii) segmented convex hull, and (iii) slicing-volume estimation. The first two approaches have been described by Auat Cheein et al. (2015) for orchard trees. In the third approach, canopy volume was calculated by segmenting the plant point cloud into a number of horizontal point cloud slices of equal thickness (1 mm). Each point cloud slice of the strawberry canopy was analysed by determining the boundary polygon. The area of the boundary was calculated for each slice and multiplied by its height achieving the volume estimation of each slice, whereas the sum provided the plant volume.

RESULTS

The volume estimation approaches were applied to the temporal strawberry point cloud dataset and found largest volumes for convex hull, followed by segmented convex hull and slicing-volume estimation method. It can be assumed that the cylindrical approach for determining the reference volume produces a bias, since the the method considers plants as a cylinder, regardless of the irregular shape of the canopy. At first measuring date, average canopy volumes were found to be 8994 cm³, 5741 cm³, 2984 cm³ and 320 cm³ for cylindrical, convex hull, segmented convex hull and slicing-volume estimation methods, respectively. After 12 weeks, the volume of the same strawberry plants was enhanced to 10515 cm³, 7347 cm³, 4480 cm³ and 352 cm³ for cylindrical, convex hull, segmented convex hull and slicing-volume estimation methods, respectively. The results showed a gradual increase in volume, which was non-invasively and repeatably obtained by analysing temporal LiDAR point cloud data. Also, it was revealed that slicing-volume estimation can removes the volumes associated with gaps and holes in the strawberry canopies. Finally, LiDAR-estimated strawberry canopy volume information can be utilized for application of plant inputs.

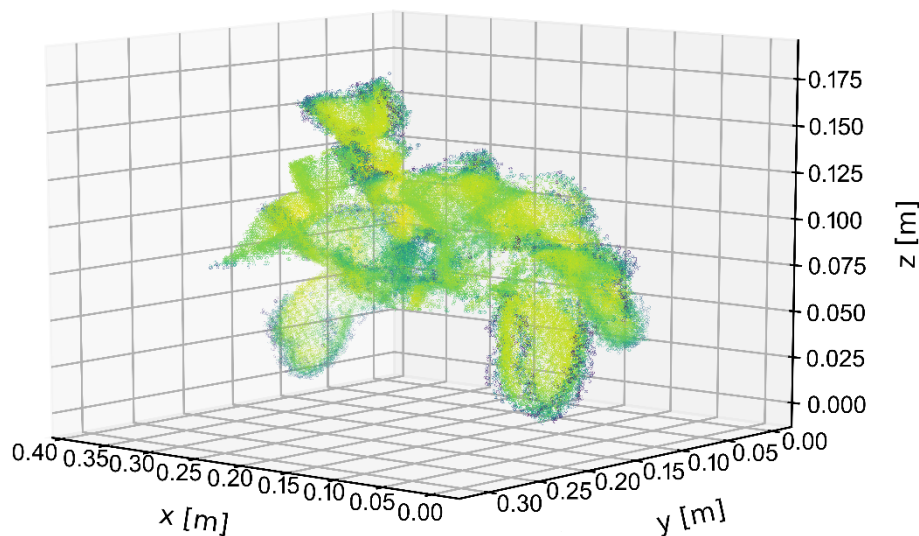


Figure 1: 3D point cloud of strawberry plant eight weeks after planting.

REFERENCES

- Auat Cheein, F. A., Guivant, J., Sanz, R., Escolà, A., Yandún, F., Torres-Torriti, M., et al. 2015. Real-time approaches for characterization of fully and partially scanned canopies in groves. *Computers and Electronics in Agriculture* 118, 361-371. <https://doi.org/10.1016/j.compag.2015.09.017>
- Tsoulias, N., Paraforos, D.S., Xanthopoulos, G., Zude-Sasse, M., 2020. Apple shape detection based on geometric and radiometric features using a LiDAR laser scanner. *Remote Sensing* 12: 2481. <https://doi.org/10.3390/rs12152481>
- Underwood, J. P., Hung, C., Whelan, B., & Sukkarieh, S., 2016. Mapping almond orchard canopy volume, flowers, fruit and yield using lidar and vision sensors. *Computers and Electronics in Agriculture*, 130, 83-96. <https://doi.org/10.1016/j.compag.2016.09.014>
- Yan, Z., Liu, R., Cheng, L., Zhou, X., Ruan, X., & Xiao, Y., 2019. A concave hull methodology for calculating the crown volume of individual trees based on vehicleborne LiDAR data. *Remote Sensing*, 11(6), 623. <https://doi.org/10.3390/rs11060623>

AN APPROACH TO SEGMENT WOOD STRUCTURE USING LIDAR SCANNER IN APPLE TREES

N. Tsoulas, M. Penzel, M. Zude-Sasse

Leibniz Institute for Agricultural Engineering and Bioeconomy (ATB), Dept. Horticultural Engineering, Potsdam, Germany

Email: ntsoulas@atb-potsdam.de

INTRODUCTION

In fruit trees, the characterization of canopy geometric features can provide indicators for the tree growth, fruit quality and yield. Among others, leaf area (LA) is one of the most important geometrical parameters due to the indirect relation with crop load and fruit size. The LA can be determined manually. However, the method is laborious, costly and destructive. Compared to arable crops, development of perennial fruit trees takes place in three dimensions (3D) and may adapt to the growing location (Zude-Sasse et al., 2016). In recent years, the assessment of canopy geometry of tree crops has been facilitated through the development of light detection and ranging (LiDAR) sensors mounted frequently on terrestrial platforms to produce the 3D point cloud of trees. Several studies have exploited the potential of LiDAR systems to extract LA and volume from a 3D point cloud at one growth stage (Sanz et al., 2018) and during seasonal tree development (Chakraborty et al., 2019). However, the utilization of such systems for estimating the LA usually includes points from woody parts, resulting in an overestimation of LA values. The objective of this study was to propose a methodology of detecting and segmenting wood points from an apple tree point cloud to improve the estimation of LA.

MATERIALS AND METHODS

The experiment was conducted in 12 trees of a commercial apple orchard (3 ha), Brandenburg, Germany, in 2020. The orchard was planted in 4 x 1 m distance with *Malus x domestica* ‘Gala’ strain ‘Baigent’ (Brookfield®). A LiDAR scanner with real time kinematic global navigation satellite system to geo-reference the data and inertial measurement unit to acquire orientation of the scanner were mounted on a tractor to scan the three-dimensional tree point cloud 5 days after full bloom (DAFB₅) and at cell division 38 DAFB (DAFB₃₈). A metal frame mounted on a tractor was used to carry the sensors along the tree rows. In both stages, trees (n = 12) were defoliated to build a regression equation of the laser hits per tree and LA. Also, the lengths of all shoots and stem were measured. A cylindrical boundary was projected around the stem position of tree point cloud, aiming at the initial segmentation of the tree point cloud. The soil was removed using random sample consensus algorithm, considering only points above 0.2 m in the analysis. The geometric feature of linearity (L) and apparent reflectance intensity (R_{ToF}) derived from a 3D point cloud were used to extract points of woody parts from points per tree (PPT) of each segmented apple tree for both growth stages (Tsoulas et al., 2020). For this purpose, k-nearest neighbour classification method was performed on each segmented tree to analyse the local neighborhood of points in 3D. Linearity and reflectance thresholds of wood points were determined based on defoliated tree at DAFB₅. The wood clusters in foliated trees were validated by the defoliated trees, which were considered as ground truth labels.

RESULTS

The probability density patterns of R_{ToF} for wood ranged between 35 % and 70 % at DAFB₅, while a broader range was observed at DAFB₃₈. The most frequent (mode) value appeared at 62 % and 40 % in 2018 and 2019, respectively. The probability density patterns of L for wood were partly overlapped in both seasons, revealing a similar mode value at 51 % and 47 % in DAFB₅ and DAFB₃₈, respectively. Mode values of R_{ToF} and L were applied as thresholds to

segment points belonging to woody parts of the canopy of each tree. Consequently, the LA estimation of all trees was done after filtering points representing wood surfaces (Figure 1). The remaining points per tree were related with the manually measured LA, indicating a $R^2 = 0.83$ at DAFB₅ and $R^2 = 0.86$ at DAFB₃₈. On the other hand, the length of stem was correlated with the manual measurements at DAFB₅ ($R^2 = 0.90$) and DAFB₃₈ ($R^2 = 0.85$). The algorithm resulted in maximum values of 82.5 % precision, 85.7 % of accuracy, 87 % recall and 86.3 % F1 score at DAFB₅, Whereas, less pronounced values of precision (79.5 %), accuracy (83.2 %), recall (82.5 %) and F1 score (80.9 %) were indicated in DAFB₃₈.

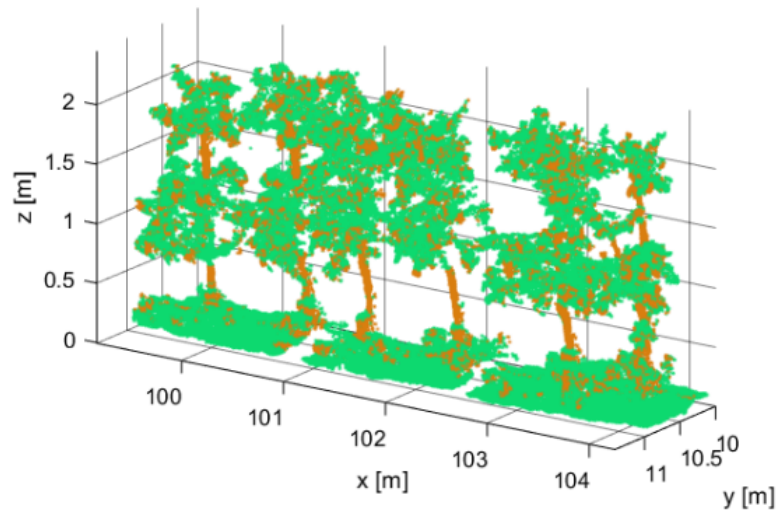


Figure 1: 3D point cloud of apple trees at DAFB38, when mature canopies appeared.

REFERENCES

- Chakraborty, M., Khot, L.R., Sankaran, S., Jacoby, P.W., 2019. Evaluation of mobile 3D light detection and ranging based canopy mapping system for tree fruit crops. *Computers and Electronics in Agriculture* 158, 284–293. <https://doi.org/10.1016/j.compag.2019.02.012>
- Sanz, R., Llorens, J., Escolà, A., Arnó, J., Planas, S., Román, C., et al., 2018. LIDAR and non-LIDAR-based canopy parameters to estimate the leaf area in fruit trees and vineyard. *Agriculture and Forestry Meteorology* 260-261 229-239 <https://doi.org/10.1016/j.agrformet.2018.06.017>
- Tsoulias, N., Paraforos, D.S., Xanthopoulos, G., Zude-Sasse, M., 2020. Apple shape detection based on geometric and radiometric features using a LiDAR laser scanner. *Remote Sensing* 12 (15) 2481 <https://doi.org/10.3390/RS12152481>
- Zude-Sasse, M., Fountas, S., Gemtos, T.A., Abu-Khalaf, N., 2016. Applications of precision agriculture in horticultural crops. *European Journal Of Horticultural Science* 81, 78–90. <https://doi.org/10.17660/eJHS.2016/81.2.2>

AN APPROACH FOR THE USE OF RGB-DEPTH PERCEPTION FOR PRUNING VINEYARD ESTIMATION

Rueda-Ayala V.¹, Moreno H.², Ribeiro A.², Andujar D.²

¹*Norwegian Institute of Bioeconomy Research, Postvegen 213, Klepp Stasjon, 4353, Norway*

²*Centre for Automation and Robotics, CAR-CSIC, Arganda del Rey, Madrid, 28500, Spain;*

d.andujar@csic.es

INTRODUCTION

On-ground assessment of geometrical features of vineyards is of vital importance to generate valuable information that can enable producers to take the optimum actions in terms of agricultural management. RGB cameras are considered the most common optical sensors in plant reconstruction for agricultural purposes. They have been widely used to evaluate phenotypic traits. RGB cameras in combination with software recognition are able to differentiate other vegetation from vineyard crops and specific parameters, such as grapes or stress factors, e.g., diseases. The information obtained can be used for extracting different vegetation indices and the creation of 3D models. A vineyard color model could describe micro-crop structure, if images are acquired at a very close range to the plants. If the assessment is based on an unmanned aerial vehicle, the 3D model can describe the macro-structure. Within RGB systems, depth cameras (RGB-D) such as the Microsoft Kinect sensor (Redmond, WA, USA) have been applied to precision agriculture purposes (Andujar et al., 2019). The Kinect v2 is a commercial videogame controller device for the Xbox game console. However, its use has been extended to many experiments or automatic platforms to apply its functioning principle to a wide array of fields beyond video gaming. The system has demonstrated its capability to scan and reconstruct 3D models of vineyards on large areas, at different times of the year and under uncontrolled daytime light, on board of an automatic platform (Bengochea-Guevara, et al. 2018). The creation of 3D models of branches is of crucial importance for further management planning. Volume and structural information can improve pruning systems, which can increase crop yield and improve crop management. In this experiment, a self-developed platform was used to reconstruct 3D models which were used to determine branch volume on several vineyard-cropping systems. The results were compared with dry biomass ground truth-values.

MATERIALS AND METHODS

A non-destructive measuring technique was implemented to assess major geometrical traits of vines, based on measurements recorded by an RGB-D camera mounted on a mobile platform (Figure 1). It was intended to evaluate the performance of RGB-D cameras as a reliable system to reconstruct 3D architecture of vines, in regard to different pruning practices. Field measurements were made in January 2020 using a mobile platform equipped with the Kinect v2 commercial sensor. The vehicle was driven in a straight line, parallel to the vine row. The Kinect v2 sensor was placed on a height-adjustable bar in front of the platform oriented to the crop. The sampling platform was driven at a constant speed of 3 km h⁻¹. Afterwards, 3D clouds were processed and filtered to create a solid volume. The algorithm reconstructs large regions using the fusion of different overlapped depth images. It stores information only on the voxels closest to the detected object (Curless and Levoy, 1996). This information is used to estimate the position and orientation of the camera while scanning. A ray is directed from the camera for each pixel of the input depth image to define the voxels in the 3D scene that cross each ray. For 3D model creation, a modified version of the iterative closest point (ICP) algorithm (Chen and Medioni 1992) was set up to estimate the position and orientation of the Kinect v2 sensor.



Figure 1: (a) Electric mobile platform comprising Kinect v2 sensor. (b) RGB section of the crop. (c) Depth image of the crop

RESULTS

For this study, different types of training systems which correspond to different forms of pruning were assessed. Vines were placed with an approximate spacing of 1 m between plants and 2 m of inter-row distance. The Kinect v2 system on-board the on-ground vehicle was capable of producing precise 3D point clouds of the evaluated pruning systems: Guyot unilateral, Cordon Royat, Pergola, Cortina, Smart Dyson, Long GDC, Scott, T-Trellis, Minimum, Govelet and vertical. Correlations of Kinect-based branch volume against pruning weight (dry biomass) resulted in high coefficients of determination ($R^2=0.85$ to $R^2=0.7$) for narrow pruning systems, while the higher volume pruning system showed lower determination coefficients. The Kinect v2 has high potential as a 3D sensor in agricultural applications for proximal sensing operations, benefiting from its high frame rate, low price in comparison with other depth cameras and high robustness.

ACKNOWLEDGMENTS

This research was funded the Spanish Agencia Estatal de Investigación (AEI) and Fondo Europeo de Desarrollo Regional (FEDER) (AGL2017-83325-C4-3-R).

REFERENCES

- Andújar, D.; Moreno, H.; Bengochea-Guevara, J.M.; de Castro, A.; Ribeiro, A. 2019. Aerial imagery or on-ground detection? An economic analysis for vineyard crops. *Computers and Electronics in Agriculture*. 157, 351–358.
- Bengochea-Guevara, J.M.; Andújar, D.; Sanchez-Sardana, F.L.; Cantuña, K.; Ribeiro, A. 2018. A Low-Cost Approach to Automatically Obtain Accurate 3D Models of Woody Crops. *Sensors*. 18, 30.
- Curless, B.; Levoy, M. 1996. A volumetric method for building complex models from range images. In *Proceedings of the 23rd Annual Conference on Computer Graphics and Interactive Techniques*, Association for Computing Machinery, New Orleans, LA, USA, pp 303–312.
- Chen, Y.; Medioni, G. 1992. Object modelling by registration of multiple range images. *Image and Vision Computing*. 10, 145–155.

ESTIMATING OCCLUDED GRAPE BUNCHES USING IMAGE ANALYSIS – CASE STUDY WITH CV. ‘ARINTO’

G. Victorino^{1,2}, R. Braga¹, J. Santos-Victor², C. M. Lopes¹

¹LEAF, Instituto Superior de Agronomia, Universidade de Lisboa, Tapada da Ajuda, 1349-017 Lisboa, Portugal

²ISR, Instituto Superior Tecnico, Universidade de Lisboa, Lisboa, Portugal

Corresponding author: Gonçalo Victorino, E-mail: gvictorino@isa.ulisboa.pt

POSTER ABSTRACT

Vineyard yield has a high temporal and spatial variability, making it hard for vine growers to predict the amount of fruit at harvest. A timely and accurate yield estimation is extremely valuable for the entire grape and wine production chain as it provides several logistic and management advantages. At farm level, vineyard yield estimation is mainly performed through laborious and often inaccurate methods that involve destructive bunch sampling. Recently, automatic fruit recognition through image analysis has been successfully explored on grapevine images. However, these methods rely on bunch exposure to the camera, which depends on canopy density at cluster zone. Thus, a great part of previous research work involves the artificial defoliation of vines to increase fruit visibility prior to image collection. The aim of our work is to explore the relationship between empty spaces in the canopy at fruit zone (canopy porosity – POR) and the percentage of visible bunch area (pvBA) to estimate the fraction of occluded bunches in full canopy grapevine images. The present work is an update on the models previously developed in Victorino et al. (2019).

An experiment was set with the white cv. ‘Arinto’, trained to a vertical shoot positioned trellis system. Data was collected near harvest from 2019 season in an experimental vineyard located in Lisbon, Portugal. Images were collected from vines with different defoliation intensities, to simulate a wide range of vegetative vigor and senescence. POR pixels were extracted along with visible bunch pixels (vBA) and were then combined into the variable GPOR ($GPOR = (POR_{\text{pixels}} + vBA_{\text{pixels}}) / \text{total}_{\text{pixels}}$). vBA was converted into pvBA using the total bunch pixels (tBA) obtained from the same vines, after being fully defoliated. A regression model was fitted to estimate pvBA using GPOR as the independent variable (Fig. 1).

Finally, tBA was computed using the estimated pvBA and original vBA, according to the equation 1: $tBA_{\text{est}} = vBA + vBA \cdot (1 - pvBA)$.

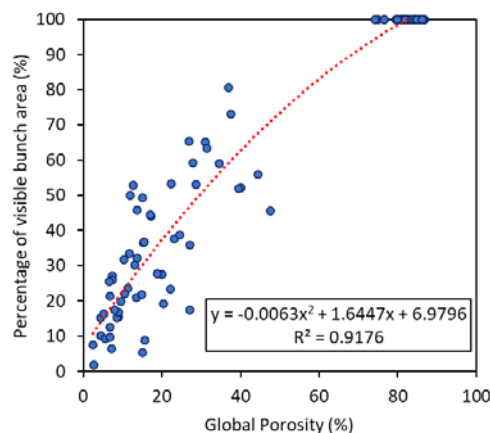


Table 1. Validation

bias	-1.0
MAE	5.9
MA%E	0.2
RMSE	8.3
RRMSE	0.2

Figure 1: Polynomial regression of pvBA over GPOR, with respective equation and resulting R^2 , fitted with the training set ($n = 86$) [left]. Table 1: statistical metrics for model validation (calculated on an independent validation set, $n = 34$). Metrics calculated according to Wallach et al. (2006) [right].

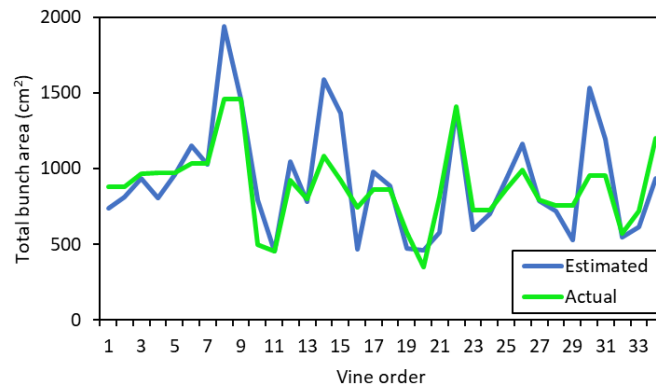


Figure 2: Comparison between estimated and actual tBA on the validation set.

In natural conditions, leaves occluded an average of 67.2% of the total bunch projected area. The regression model presented a high and significant R^2 showing that GPOR can effectively explain a high portion of pvBA variability (fig. 1), slightly higher than if only POR was used. Model validation with an independent dataset ($n = 34$) showed a very low underestimation tendency of the model (negative bias), with a MA%E close to zero and a RMSE of 8.3 pvBA.

Total estimated bunch area, including occluded bunches, was calculated using equation 1. The actual accumulated tBA of the 34 vines, after being converted to m^2 , was $29.9 m^2$, while the estimated one was $31.3 m^2$, resulting in a final relative error of 4.7%, 7% lower than when using POR exclusively. Visual observation of the individual cases shows a good relationship between estimated and actual values (fig. 2).

Our results indicate that canopy porosity presents promising results towards estimating the percentage of bunches that are occluded by leaves in different scenarios of vegetative vigor. This approach is even more effective when the initial visible bunch area is also considered as a canopy blank space. Work is currently ongoing towards improving the models with other image-based variables and generalizing this methodology to other cvs. and vineyard conditions.

Key words: canopy porosity; grapevine; hidden fruits; vineyard yield estimation; proximal sensing

REFERENCES:

Victorino, G., Maia, G., Queiroz, J., Braga, R., Marques, J., Santos-Victor, J., & Lopes, C. (2019). Grapevine yield prediction using image analysis - improving the estimation of non-visible bunches. *Digitizing Agriculture*.
 Wallach, D., Makowski, D., Jones, J. W., & Brun, F. (2006). Working with dynamic crop models: evaluation, analysis, parameterization, and applications. Elsevier.

HYPERSPECTRAL IMAGING AND MACHINE LEARNING FOR PEST AND DISEASE DETECTION IN COMMERCIAL VINEYARDS

Hernández I.¹, Gutiérrez S.², Alonso M.¹, Ceballos S.¹, Iñiguez R.¹, Palacios F.¹, Diez-Navajas A. M.³, Tardaguila J.^{1*}

¹*Televitis Research Group. University of La Rioja, 26007 Logroño, Spain,*

²*Department of Computer Science and Artificial Intelligence, University of Granada, 18071 Granada, Spain,*

³*Department of Plant Production and Protection, NEIKER-Basque Institute for Agricultural Research and Development, Basque Research and Technology Alliance (BRTA), Campus Agroalimentario de Arkaute s/n, 01192 Arkaute, Spain*

*Corresponding email: javier.tardaguila@unirioja.es

ABSTRACT

Pests and diseases such as spider mite and downy mildew severely affect grapevines. Fast and objective methods for their detection in commercial vineyards are needed. In this work, hyperspectral imaging, computer vision and machine learning were used to detect spider mite and downy mildew symptoms in grapevine leaves. An accuracy of 93.2% and an F1-score of 0.92 were obtained in the classification of leaf disks using a model trained with support vector machines. This work holds out the possibility of using non-invasive technology and machine learning for the detection of diseases and pests in viticulture.

INTRODUCTION

Pests and diseases have a high impact on yield and grape quality in viticulture (Galet, 1996), and their identification is time-consuming and requires trained personnel. New non-invasive sensing technologies and artificial intelligence could be used for pest and disease detection in grapevine (Cruz et al., 2019; Zhu et al., 2020). The aim of this work was to use hyperspectral imaging, computer vision and machine learning for automatic detection of spider mite (pest) and downy mildew (disease) symptoms in commercial vineyards.

MATERIALS AND METHODS

Grapevine leaves infected with spider mite (*Eotetranychus carpini*) and downy mildew (*Plasmopara viticola*) and non-infected leaves were collected in a commercial vineyard (*V. L. cv. Hondarribi Zuri Zerratia*) located in northern Spain. Hyperspectral images of leaf disks were taken under laboratory conditions with the Resonon Pika L VNIR camera, capturing the visible and near-infrared (VNIR, 400-1000 nm) range.

Image processing was carried out to obtain a representative spectrum from each disk using computer vision techniques and machine learning (Figure 1). First, hyperspectral images (Figure 1A) were pre-processed using reflectance transformation, Savitzky-Golay filtering and Z-score normalization. Then, leaf disk spectrums were separated from the background spectrums classifying spectrums of each image with a support vector machine (SVM) model (Figure 1B). Then, from the binary images (the result of classifying between leaf spectrum and non-leaf spectrum), erosion and dilation morphological transformations were applied to remove small holes and smooth the borders of the disks. Finally, the watershed segmentation algorithm (Vincent & Soille, 1991) was applied to separate the disks in each image (Figure 1C).

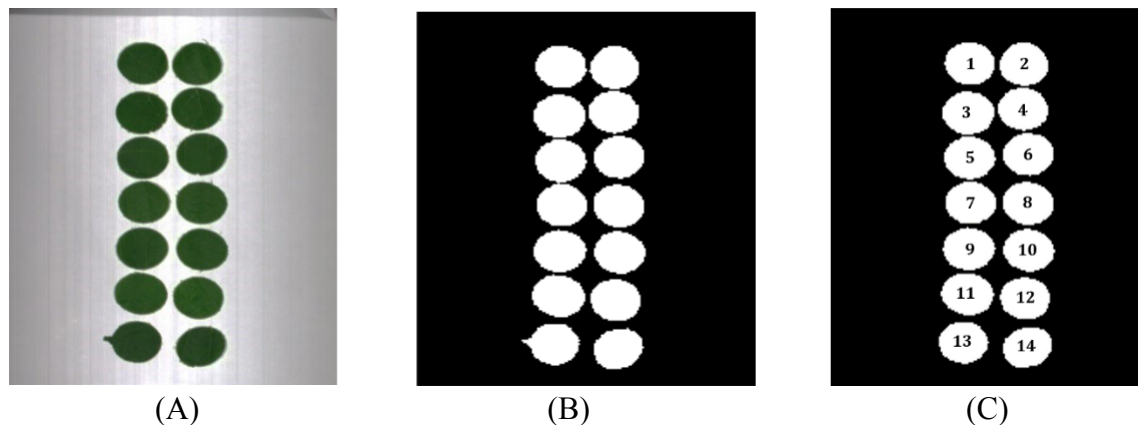


Figure 1. (A) Example of original image, (B), leaf separation from background with an SVM model and (C) leaf disk location with watershed.

The average spectrum of each leaf disk were classified into disks with downy mildew symptoms, with spider mite symptoms or healthy using a different SVM model. Stratified 5-fold cross-validation was applied and accuracy and F1-score metrics were used to analyze the results.

RESULTS AND DISCUSSION

An accuracy of 93.2% and an F1-score of 0.92 were obtained in the classification of leaf disks with spider mite symptoms, with downy mildew symptoms and without symptoms. This considerable accuracy demonstrates the capability of the trained model for the automated downy mildew and spider mite detection and their differentiation in grapevine. The results show that hyperspectral imaging and artificial intelligence can be used for identifying key diseases and pests in phytopathology and crop protection. This work opens the window for the application of non-invasive techniques and machine learning for disease and pest detection and differentiation in commercial vineyards.

ACKNOWLEDGEMENTS

This work has been developed as part of the project NoPest (Novel Pesticides for a Sustainable Agriculture), which received funding from the European Union Horizon 2020 FET Open program under Grant agreement ID 828940.

REFERENCES

- Cruz, A., Ampatzidis, Y., Pierro, R., Materazzi, A., Panattoni, A., De Bellis, L., et al. (2019). Detection of grapevine yellows symptoms in *Vitis vinifera* L. with artificial intelligence. *Computers and Electronics in Agriculture*, 157, 63–76. <https://doi.org/10.1016/j.compag.2018.12.028>
- Galet, P. (1996). Grape diseases. Chaintre, France: Oeno Plurimedia.
- Vincent, L., & Soille, P. (1991). Watersheds in digital spaces: an efficient algorithm based on immersion simulations. *IEEE Transactions on Pattern Analysis and Machine Intelligence*, 13(6), 583–598. <https://doi.org/10.1109/34.87344>
- Zhu, J., Wu, A., Wang, X., & Zhang, H. (2020). Identification of grape diseases using image analysis and BP neural networks. *Multimedia Tools and Applications* 79 14539–14551 <https://doi.org/10.1007/s11042-018-7092-0>

IN-FIELD DOWNY MILDEW DETECTION IN GRAPEVINE USING COMPUTER VISION AND CONVOLUTIONAL NEURAL NETWORKS

Hernández I.¹, Gutiérrez S.², Ceballos S.¹, Iñiguez R.¹, Palacios F.¹, Diez-Navajas A. M.³, Tardaguila J.^{1*}

¹*Televitis Research Group. University of La Rioja, 26007 Logroño, Spain,*

²*Department of Computer Science and Artificial Intelligence, University of Granada, 18071 Granada, Spain,*

³*Department of Plant Production and Protection, NEIKER- Basque Institute for Agricultural Research and Development, Basque Research and Technology Alliance (BRTA), Campus Agroalimentario de Arkaute s/n, 01192 Arkaute, Spain*

*Corresponding email: javier.tardaguila@unirioja.es

ABSTRACT

Downy mildew is a key disease in grapevine and its detection in commercial vineyards is needed. Artificial intelligence could help to achieve automated and accurate detection of this disease. In this work, computer vision and deep learning techniques were applied to detect downy mildew on grapevine leaves under field conditions. An accuracy of 91.4% was obtained using a convolutional neural network. Promising results are shown in the use of non-invasive technologies and convolutional neural networks for disease detection in viticulture.

INTRODUCTION

Downy mildew is a very relevant disease in many commercial crops as it can cause a serious impact to yield (Martínez-Bracero et al., 2019). Currently, disease detection and monitoring are time-consuming and require trained personnel. Deep learning and computer vision are used for disease and pest detection in agriculture (Barbedo & Garcia, 2019; Chen et al., 2020), and this opens a window for its application in the automated detection of downy mildew. This work aimed to automatically detect downy mildew symptoms in grapevine leaves under field conditions using computer vision and deep learning.

MATERIALS AND METHODS

RGB images of grapevine canopy with and without symptoms of downy mildew (*Plasmopara viticola*) were taken in a commercial vineyard (*Vitis vinifera* L. cv. Hondarribi Zuri Zerratia) located in northern Spain. RGB images were manually taken under natural daylight conditions using a Canon EOS 5D Mark IV digital camera.

Computer vision techniques were used to remove the background from images and to highlight the visual features of symptoms (Figure 1). Grabcut segmentation method (Rother et al., 2004) was used to remove the background of the images. The number of images for classification was increased using data augmentation to train more robust classification models, creating new images from the originals by changing brightness, height and width shifts, horizontal and vertical flips, and small rotations. Leaf zones that could potentially represent downy mildew symptoms were highlighted using the HSV (Hue, Saturation, Value) colour space, considering only pixels with yellowish or reddish colours.

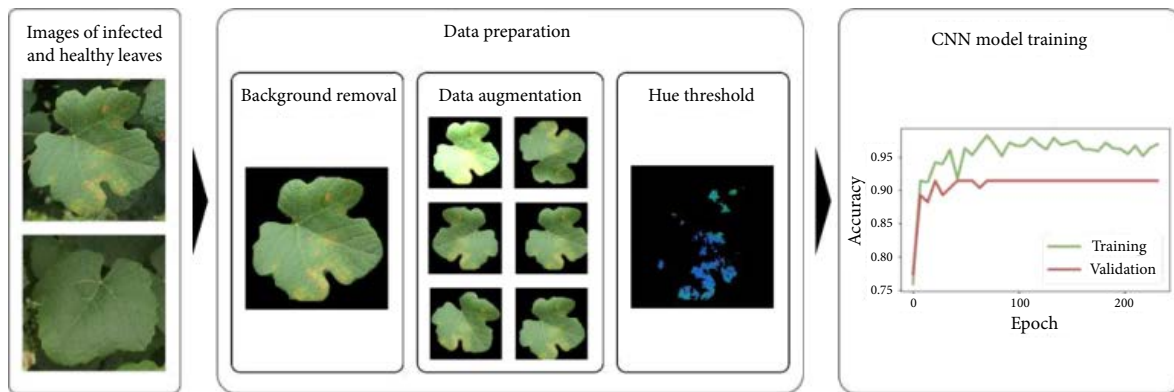


Figure 21: Diagram of the steps followed in this work. Grapevine leaf images with and without downy mildew symptoms were acquired. Data were prepared by background removal, data augmentation and hue threshold. Classification of data was made with a convolutional neural network (CNN).

Leaf images were classified into infected and non-infected classes using a CNN model. Hold-out validation was employed for the analysis of the classification results, using accuracy as metric.

RESULTS AND DISCUSSION

An accuracy of 91.4% was obtained in the hold-out validation. The results prove the efficiency of the trained model in the detection of downy mildew symptoms in grapevine leaves. Computer vision techniques were useful for feature extraction from images, standing out the relevant pixels of the images. On the other hand, deep learning helps to create a robust model capable of providing a fast and accurate classification of downy mildew symptoms in commercial vineyards. This work demonstrates the usefulness of non-invasive technologies and artificial intelligence for disease detection in plants under field conditions.

ACKNOWLEDGEMENTS

This work has been developed as part of the project NoPest (Novel Pesticides for a Sustainable Agriculture), which received funding from the European Union Horizon 2020 FET Open program under Grant agreement ID 828940.

REFERENCES

- Barbedo, A., & Garcia, J. (2019). Plant disease identification from individual lesions and spots using deep learning. *Biosystems Engineering*, 180, 96–107. <https://doi.org/10.1016/j.biosystemseng.2019.02.002>
- Chen, J., Chen, J., Zhang, D., Sun, Y., & Nanekaran, Y. A. (2020). Using deep transfer learning for image-based plant disease identification. *Computers and Electronics in Agriculture*, 173, 105393. <https://doi.org/10.1016/j.compag.2020.105393>
- Martínez-Bracero, M., Alcázar, P., Velasco-Jiménez, M. J., & Galán, C. (2019). Fungal spores affecting vineyards in Montilla-Moriles Southern Spain. *European Journal of Plant Pathology*, 153(1), 1–13. <https://doi.org/10.1007/s10658-018-1532-6>
- Rother, C., Kolmogorov, V., & Blake, A. (2004). “GrabCut” - Interactive foreground extraction using iterated graph cuts. *ACM Transactions on Graphics*, 23(3). <https://doi.org/10.1145/1015706.1015720>

EVALUATING THE POTENTIAL OF POTATO YIELD MAPPING USING HIGH SPATIAL AND TEMPORAL RESOLUTION PLANETSCOPE SATELLITE IMAGES

Mizuta K.¹, Miao Y.¹, Lacerda L.N.¹, Rosen C.¹, Gupta S.¹, Kang S.K.¹, Huang Y.²

¹*University of Minnesota, St. Paul, MN, USA.*, ²*Crop Science Research Laboratory, USDA-ARS, Mississippi State, MS, USA*

Accurate high-resolution yield maps are necessary to identify spatial yield variability patterns within commercial fields, determine the key factors affecting yield and finally provide insights for management practice in precision agriculture. However, existing systems for monitoring potato yield can easily lead to improper interpretation of on-farm yield variability. The main reasons lie in procedures for data collection and processing, such as improper calibration settings in harvest sensor, incomplete separation of attached soil and potatoes, errors in operation of harvest sensor and data processing/cleaning. To produce accurate and reliable potato yield maps, alternative technologies need to be developed.

Remote sensing technology has been extensively applied for in-season crop health monitoring (e.g., leaf area index, biomass, diseases/pests) and yield prediction (Miao and Mulla 2016). Generally, vegetation indices calculated from remote sensing images are used to correlate to yield variability through statistical and machine learning models. Previous potato yield prediction studies with remote sensing have indicated that the methodology is effective for crop yield prediction and pattern analysis (Gómez et al. 2019; Newton et al. 2018). Particularly, multiple temporal remote sensing monitoring across the growing season can uniquely offer insights into tuber development processes and identify the limiting factors such as soil-landscape conditions, water and nutrient management.

PlanetScope (Planet Team, 2018) is a newly available commercial cube satellite platform that offers daily multispectral imagery for any location in the world. Approximately 130 Planet Labs Dove cube satellite sensors have been launched into sun-synchronous low earth orbit. This orbit path and inclination allow for daily revisit time of any point on earth between 9:30 and 11:30 AM solar time. The satellite data contains four bands (blue: 455–515 nm; green: 500–590 nm; red: 590–670; and near-infrared (NIR): 780–860 nm). The spatial resolution is about 3m. Little has been reported for potato yield mapping using PlanetScope satellite images. Therefore, the objective of this study was to evaluate the potential of using PlanetScope satellite images for predicting potato yield.

In the current study, a commercial potato field near Becker, MN, USA was selected as an experimental site. To better select the most representative sites for spatial yield variability for ground sampling and validation, the conditional Latin hypercube sampling (cLHS) by integrating all features of environment, agronomy and remote sensing monitoring was used to select 50 ground-truth sampling sites for yield measurement in the potato field. Total potato tubers from five hills were collected at each site by hand digging and weighed at the end of the sampling day. The yield was calculated based on 3 m within-row hill spacing and 0.9 m row spacing. In-season PlanetScope images were obtained six times during crop growth dates in 2020 (i.e., June 25, June 27, July 12, July 24, August 4 and August 11). Several vegetation indices were calculated, including green normalized difference vegetation index (GNDVI), normalized difference vegetation index (NDVI), soil-adjusted vegetation index (SAVI) and modified simple ratio (MSR). In addition to multiple linear regression (MLR) models, prediction models were constructed using two machine learning algorithms (random forest, RF; and support vector machine, SVM) to predict potato yield (Zha et al. 2020). The RF and SVM models

were developed using the statistical software *R* (4.0.4) packages, “caret” and “randomForest.” The agreement between the observed and the predicted potato yield was evaluated using the coefficient of determination (R^2) and root-mean-square error (RMSE) in prediction. The models with the largest R^2 and lowest RMSE in prediction were recognized.

Potato tuber yield varied across the field from 33 to 105 t ha⁻¹. Preliminary results indicated that multiple linear regression using all VIs from different dates achieved the highest R^2 (=0.70), while sub-setting data into training (70%) and testing (30%) datasets resulted in the highest adjusted R^2 (=0.53). More analyses are being performed to use machine learning models to improve potato yield prediction and will be presented in the poster.

- Gómez, D., Salvador, P., Sanz, J., and Casanova, J. L. (2019). Potato Yield Prediction Using Machine Learning Techniques and Sentinel 2 Data. *Remote Sensing*, 11(15), 1745. <https://doi.org/10.3390/rs11151745>
- Miao, Y., and Mulla, D. J. (2016). Precision farming. In P. S. Thenkabail (Ed.), *Land Resources Monitoring, Modeling, and Mapping with Remote Sensing*. Boca Raton, FL, USA: CRC Press.
- Newton, I. H., Tariqul Islam, A. F. M., Saiful Islam, A. K. M., Tarekul Islam, G. M., Tahsin, A., and Razzaque, S. (2018). Yield Prediction Model for Potato Using Landsat Time Series Images Driven Vegetation Indices. *Remote Sensing in Earth Systems Sciences*, 1(1), 29–38. <https://doi.org/10.1007/s41976-018-0006-0>
- Planet Team. (2018). *Planet Application Program Interface: In Space for Life on Earth*. San Francisco, CA, USA. <https://api.planet.com>
- Zha, H., Miao, Y., Wang, T., Li, Y., Zhang, J., Sun, W., et al. (2020). Improving Unmanned Aerial Vehicle Remote Sensing-Based Rice Nitrogen Nutrition Index Prediction with Machine Learning. *Remote Sensing*, 12(2), 215. <https://doi.org/10.3390/rs12020215>

OBTAINING REMOTE SENSOR DATA OF FRUIT TREES BY MEANS OF CIRCULAR CONVEYOR SYSTEM

Zude-Sasse M., Tsoulas N., Elwert S., Geyer M.

Leibniz Institute for Agricultural Engineering and Bioeconomy (ATB), Potsdam, Germany,

Email: mzude@atb-potsdam.de

INTRODUCTION

Remote sensing of fruit trees is frequently carried out by means of various platforms. The selection of the platform depends mainly on the measuring time interval required by the application (Zude-Sasse et al., 2016). Most frequently, a tractor is used for carrying the sensor along the tree rows. However, the tractor's combustion engine, elevation of terrain, and roughness of the ground may cause vibration and displacement of the sensor (Janeway, 1975). Displacement of the sensor can seldom be avoided with an active platform, but can be commonly corrected by means of a global navigation satellite system (GNSS) and inertial measurement unit (IMU). Effects of high frequency vibration on the sensor signal is usually ignored. For scientific purposes, it is desirable to obtain sensor data with reduced forced vibration from the platform, which was approached by developing a sensor platform for autonomous monitoring of fruit trees.

MATERIAL AND METHODS

A circular conveyor was developed, employing electrical engine working with 50 Hz (DRN71, SEW Eurodrive, Germany) and stainless steel chain with mechanical suspensions for various plant sensors (Fig. 1). This phenotyping platform was established in an experimental apple orchard in temperate climate, in 2020. The conveyor system enables automated monitoring of 111 apple trees (*Malus x domestica* Borkh. 'Gala' and 'JonaPrince') and pollinator trees planted in one row of 84 m length. In the trial, an inertial measuring unit (IMU), containing gyroscope and accelerometer, was employed (MTi-G-710, XSens, Enschede, Netherlands). The angular vibration was resolved in yaw, pitch and roll.

Conveyor data were compared to acceleration and vibration measured when the sensors were placed on a tractor (LSA 209P, Fendt, Marktoberdorf, Germany). The conveyor chain can move in a range of 1 – 7 m min⁻¹; in the experiment, similar velocity was adjusted to 7 min min⁻¹. Both systems were run on the same row of apple trees.

RESULTS AND DISCUSSION

Tractor low frequency vibration (0 – 20 Hz) occurs mainly vertically and can be attributed to rough ground, while high frequency vibration is caused by the combustion engine and the mass asymmetries (Loutridis et al., 2010). When the IMU was mounted on the tractor, the variance of angular vibration, measured in parallel to the tree row with 1.6 m distance to the trees was 12.780°, 0.875°, and 0.375° for yaw, roll and pitch, respectively. The values are consistent with data described in the literature. Variance of GNSS data was 16.36*10⁻⁵°, 15.40*10⁻⁶°, 32.50*10⁻²° considering latitude, longitude, altitude, respectively.

In comparison, at the stationary conveyor measured with the same geometry to the trees, marginal variance of sensor displacement was found with 1.195°, 0.533° and 0.080° for yaw, roll and pitch angles, respectively (Fig. 1b). Particularly the movement around yaw axis was marginal at the conveyor compared to tractor displacement, but also roll and pitch variance decreased at the conveyor. GNSS variance was reduced for lat. = 16.03*10⁻⁵°, long. = 14.40*10⁻⁶°, and enhanced for alt. = 35*10⁻²° compared to tractor data.

Concluding, plant sensor data, e.g. from laser scanner or camera system, can be obtained with enhanced quality at the conveyor. The marginal displacement combined with the automated

recording of sensor data should be useful for reducing the measuring uncertainties potentially occurring when moving plant sensors along the crop on an unmanned or conventional vehicle in real-world application, and, therefore, to obtain plant input data for the development of robust agronomic models.

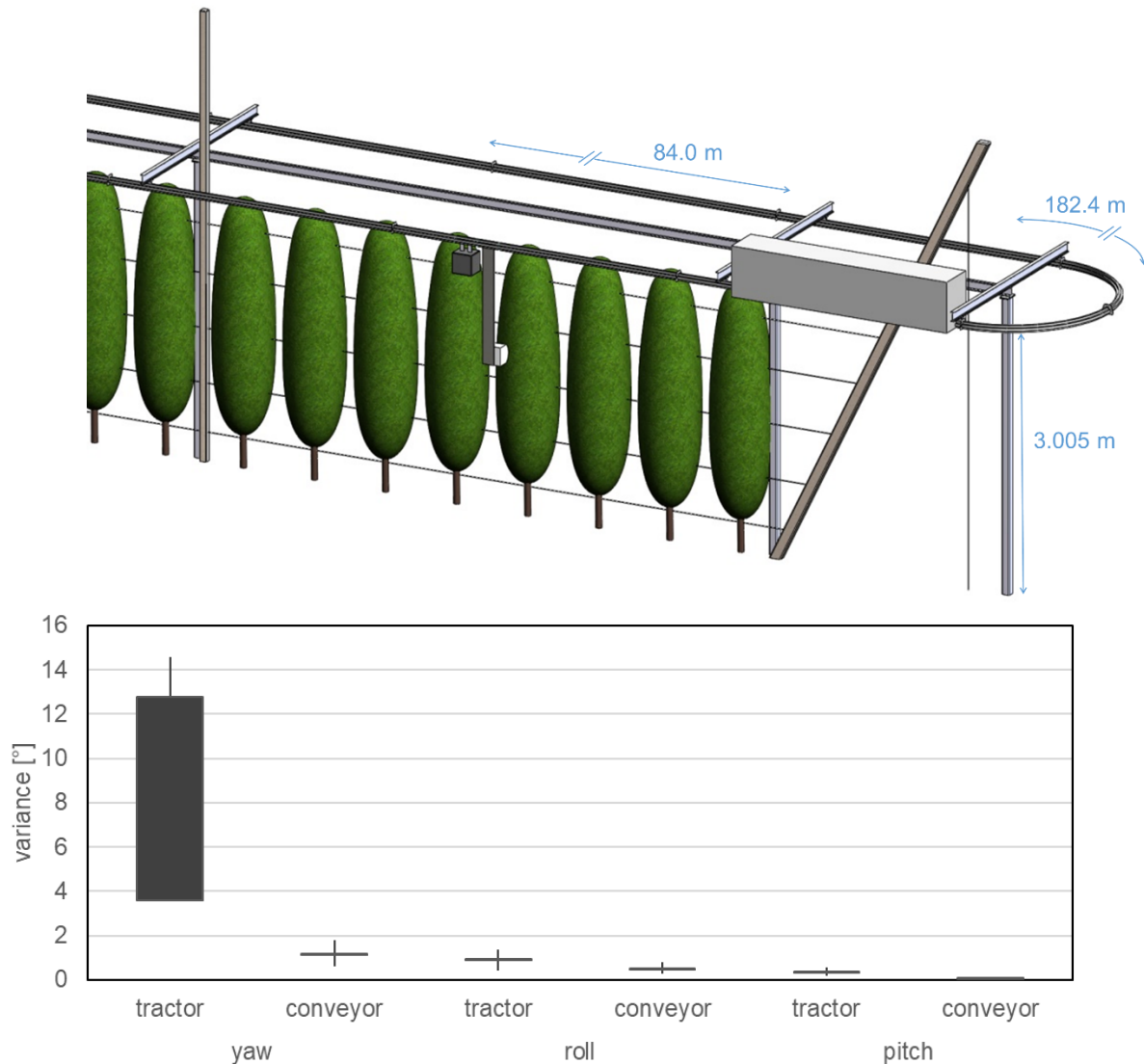


Figure 1: Schematic of circular conveyor section (upper) and variance of angular displacement measured at tractor and conveyor.

REFERENCES

- Janeway, R. (1975). Human vibration tolerance criteria and applications to ride evaluation. SAE Technical Paper 750166. <https://doi.org/10.4271/750166>
- Loutridis, S., Gialamas, T., Gravalos, I., Moshou, D., Kateris, D., Xyradakis, P., et al. (2010). A study on the effect of electronic engine speed regulator on agricultural tractor ride vibration behavior. *Journal of Terramechanics* 48: 139-147. <https://doi.org/10.1016/j.jterra.2010.10.002>
- Zude-Sasse, M., Fountas, S., Gemtos, T.A., Abu-Khalaf, N. (2016). Applications of precision agriculture in horticultural crops – review. *European Journal of Horticultural Science* 81: 78-90. <https://doi.org/10.17660/eJHS.2016/81.2.2>

BIOMASS ESTIMATIONS OF PERENNIAL RYEGRASS USING UAV-BASED MULTISPECTRAL BANDS AND VEGETATION INDICES

Pranga J.^{1,2}, Borra-Serrano I.¹, De Swaef T.¹, Aper J.¹, Ghesquiere A.¹, Roldán-Ruiz I.^{1,3}, Janssens I.², Ruyschaert G.¹, Lootens P.¹

¹*Plant Sciences Unit, Flanders Research Institute for Agriculture, Fisheries and Food (ILVO), Melle, Belgium*

²*Department of Biology, University of Antwerp, Wilrijk, Belgium*

³*Department of Plant Biotechnology and Bioinformatics, Ghent University, Ghent, Belgium*

BACKGROUND

Optimisation of agricultural monitoring and subsequent decision making is essential for precision agriculture. This is of particular importance for accurate biomass estimations that can help in grassland management, for example, in defining the optimal mowing time. Recent research (Borra-Serrano et al., 2019; Aper et al., 2019) advanced on the UAV-based non-destructive herbage yield predictions in perennial ryegrass (*Lolium perenne* L.). This study follows up on those procedures and seeks to evaluate and compare the biomass predictor potential of spectral bands and vegetation indices (VIs) derived from a ten-band multispectral (MS) camera.

MATERIALS AND METHODS

The experimental site located in Merelbeke (Belgium) comprises both diploid and tetraploid trials of perennial ryegrass. More than 200 varieties and populations were tested in two replicates (468 plots of 7.8 m² each). Biomass samples were collected on 21 and 22 September 2020 (cut 4) with a plot harvester (Haldrup F-55, Haldrup, Denmark). On 15 September, a UAV flight with a multispectral sensor (Dual Camera System, Micasense, USA) was carried out at an altitude of 30 m and 80% front and side overlap. The images obtained were processed with Pix4D Mapper 4.5.6 (Pix4D, Switzerland). In this study, dry matter yield (DMY) was predicted using two sets of variables: one on the spectral bands as such, and one on derived VIs. The MS sensor utilised comprised ten bands: coastal blue (444 nm), blue (475 nm), green (531 nm), green (560 nm), red (650 nm), red (668 nm), red edge (705 nm), red edge (717 nm), red edge (740 nm) and NIR (842 nm). A variety of VIs were derived using these calibrated reflectance bands, including NDVI, GNDVI, WDRVI, SAVI, MSAVI2, PVI, EVI, GARI, MCARI, PRI, CLg and SR described in more detail by Xue & Su (2017). Median and interquartile range (IQR) values were then extracted from the selected variables with the *v.rast.stats* tool (QGIS 3.12.3 with GRASS 7.8.3. software) for each plot. Prediction models were built with the Random Forest (RF) algorithm within the *mlr* package using RStudio v1.3.1093 (RStudio: IDE for R, R Studio Inc., USA). Model performance was assessed using the repeated nested cross-validation loop (with a total of 50 iterations). Accuracies were quantified and compared using relative root mean square error values (rRMSE).

RESULTS AND DISCUSSION

The measured DMY was 1697 kg ha⁻¹ with an SD of 376 kg ha⁻¹ and a minimum and maximum of 785 kg ha⁻¹ and 2687 kg ha⁻¹, respectively. Median spectral signatures extracted from two selected plots (both diploid genotypes) with different DMY production (Figure 1A) showed differences, especially in the red edge and the near-infrared (NIR) region. In this example, the plot with higher DMY shows higher reflectance in this part of the spectrum. Pearson correlation coefficients between DMY and red edge740 (PCC = 0.31) and NIR842 (PCC = 0.43) were the highest among tested bands (Figure 1B).

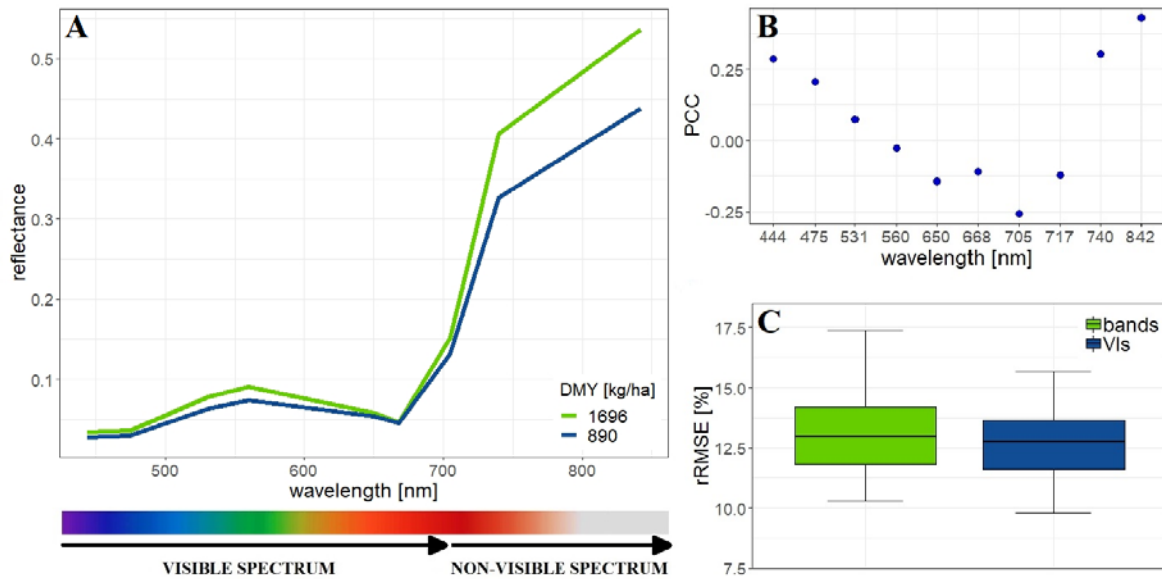


Figure 1: Comparison of (A) spectral signatures between two selected plots with different dry matter yield (DMY) production, (B) Pearson Correlation Coefficients (PCC) between tested spectral bands and DMY, (C) model accuracy boxplots for spectral-based predictor variables (bands and VIs).

Preliminary analysis of the model performance assessment (Figure 1C) showed that mean rRMSE for a dataset based on the spectral bands (13.1%) or VIs (12.8%) provided comparable results, with VIs obtaining slightly better average estimates. In terms of error distribution (i.e. precision), the standard deviation (SD) accounts for 1.7% and 1.4% for bands and VIs, respectively. The advantage of using vegetation indices in remote sensing applications and vegetation monitoring over spectral bands lies in their interpretability.

CONCLUSIONS

In general, this study has demonstrated the efficiency of the multispectral bands and vegetation indices in predicting ryegrass yield in the autumn cut. Presented findings complement those of earlier studies. Future research will focus on the applicability and performance of the model on the entire growing season, i.e. multiple cuts per year.

ACKNOWLEDGEMENTS

This study was conducted within the FutureArctic project (www.futurearctic.be) under the Marie Skłodowska-Curie grant agreement No 813114. Special thanks to Thomas Vanderstocken and Aaron Van Gehuchten for carrying out the drone flights.

REFERENCES

- Aper J., Borra-Serrano I., Ghesquiere A., De Swaef T., Roldan-Ruiz I., Lootens P., et al. (2019). Yield estimation of perennial ryegrass plots in breeding trials using drone images. *Grassland Science in Europe* 24, 312-314.
- Borra-Serrano I., De Swaef T., Muylle H., Nuyttens D., Vangeyte J., Mertens K., et al. (2019) Canopy height measurements and non-destructive biomass estimation of *Lolium perenne* swards using UAV imagery. *Grass and Forage Science*, 74(3), 356-369
- Xue, J., & Su, B. (2017). Significant remote sensing vegetation indices: A review of developments and applications. *Journal of Sensors*, 2017. <https://doi.org/10.1155/2017/1353691>

COMBINED TRAFFIC CONTROL OF IRRIGATION ON HETEROGENEOUS FIELD

A. Nagy¹, A. Szabó¹, Cs. Juhász¹, B. Gálya Farkasné¹, Á. Kövesdi² and J. Tamás¹

¹*University of Debrecen, Faculty of Agricultural and Food Sciences and Environmental Management, Institute of Water and Environmental Management 138. Böszörményi str. Debrecen H-4032, Hungary*

²*Magtár Kft. 2. Kombájn srt. Szolnok H-5000, Hungary*

Water scarcity will become a fundamental problem that will trigger changes in agricultural cultivation and management practices especially in arid and semi-arid conditions (Falkenmark 2013; Nagy et al., 2018). The trend of annual precipitation is still very uncertain in Hungary, the frequency of drought has already increased significantly strongly due to rising temperatures, and decrease in precipitation in the vegetation periods (Tamás et al., 2015; Juhász et al., 2020). Beside water retention measures, the above needs can only be met in a sustainable way with water and energy-saving irrigation, which presupposes different innovative irrigation solutions, especially in the Central European region. Groundwater, which is predominant in arid areas that are low in surface waters, is the source of irrigation water for central pivot equipment (Sui & Yan, 2017), while in this semi-arid/semi-humid region, surface water is protected to supply linear pivots. Several experiments have been made worldwide to evaluate the efficiency of variable rate irrigation (VRI), and investigate its impact on yield and soil. Based on vegetation status, management zones can be created, which can be effective in water control. The aim of the research was to develop a combined traffic control for water-saving precision sprinkler irrigation system on arable land (85 ha), which is located in the reference area of the Tisza Riven Basin. During the research, a real-time eco-potential measurement methodology for water management was developed for water-saving precision sprinkler irrigation system located in South-East Nyírség, Szabolcs-Szatmár-Bereg county in the North-Eastern region of Hungary. A Reinke 2060 PL irrigation machine with a total structural length of 209.09 m was installed in the field. The type of nozzle used is NELSON R3000, which is equipped with 100 kPa pressure regulators and is located at a height of 2.1 m from the ground. Pivoting operation and VRI operation in linear mode can be distinguished.

The precision grid-based soil sampling was carried out on an agricultural field. Different databases and maps were used to elaborate the soil sampling strategy. Core soil samples in two layers (30 cm and 60 cm) were taken. On the arable land analysed, 102 points were modelled, representing more than 1 sample per hectare (1.19 samples/ha), from a total of 510 samples. The texture and soil water retention parameters were measured to determine soil density, total available water content, gravitational water content. Soil chemical properties were also measured and were examined in the Laboratory of Soils of the University of Debrecen, Institute of Water and Environment Management. After laboratory testing, high precision soil maps and a 3-D model of deep root zone were created to support the establishing of a water saving variable rate irrigation system by selecting and identifying sites for different agro-technical implementations and precision management zones.

Irrigation water calculations for traffic control were based on total available water content. In general, it is advisable to start irrigation when the total available water content (TAW) is dropped to 60% (depletion rate 40%), so it was calculated with this value when calculating the actual moisture content. In order to calculate the amount of irrigation water, it is necessary to know the water loss in addition to the thickness of the layer to be irrigated. The water loss can be calculated based on the field capacity, the actual moisture content and the water content at

wilting point. Total available water content of the upper layer has a minimum value of 4.01% and maximum of 25.85% and with mean values of 11.14% with a standard deviation of 4.12% in the deeper layer. Lower values of available water content were also noted, the minimum was 1.95% with a maximum of 15.94% and mean values were 10.78% with a standard deviation of 4.55%. Based on the depletion rate and TAW, the amount of water loss was calculated expressed in a volumetric %, which had to be converted to mm. Since 1 V/V% means 1 mm moisture in a 10 cm thick layer, the numerical value of volumetric water content% also gives the moisture content stored in 10 cm thick layer in mm, i.e.: 1 t^o% = 1mm/10 cm. The same relation can be used if the amount of irrigation water is to be calculated in mm. Based on this, the percentage distribution of water was determined for application in creating VRI zones (Figure 1).

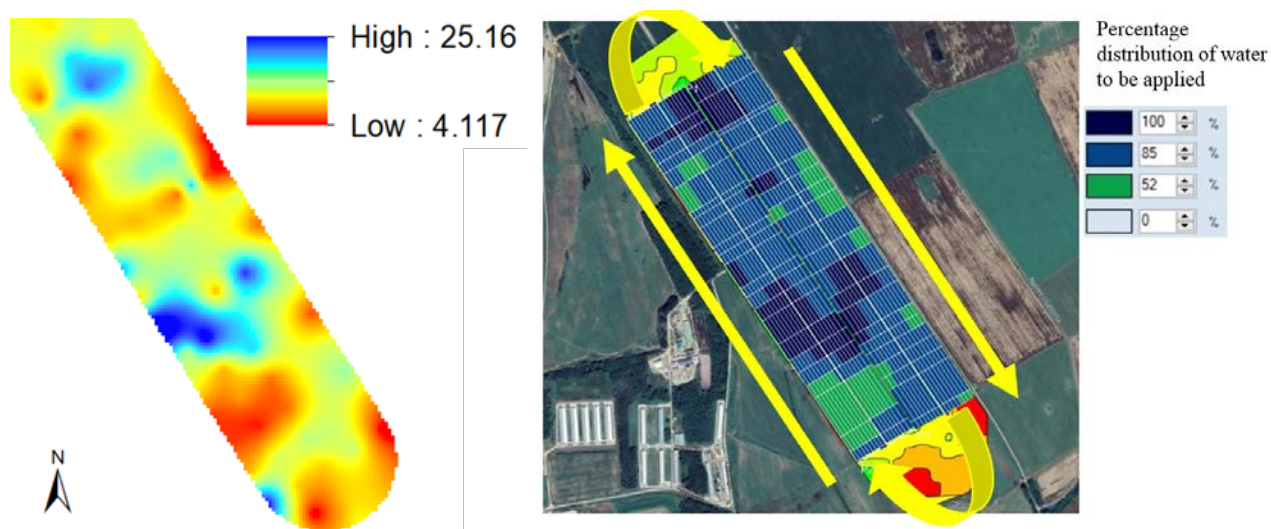


Figure 1: Available water content at 30 cm depth and VRI based traffic control on the basis of TAW (yellow arrows are the directions of the run of irrigation machine)

The research was financed by H2020 - Water retention and nutrient recycling in soils and streams for improved agricultural production’ — ‘WATERAGRI (Number 858375) project.

REFERENCES

- Falkenmark, M. 2013. Growing water scarcity in agriculture: future challenge to global water security. *Philosophical Transactions of the Royal Society A: Mathematical, Physical and Engineering Sciences*. 371. 2002, 20120410–20120410.
- Juhász, Cs., Gálya, B., Kovács, E., Nagy, A., Tamás, J. and Huzsvai, L. 2020. Predictability of weather and crop yield in regions of continental four-season climate. *Computers and Electronics in Agriculture*, 173 105400.
- Nagy, A., Fehér, J. and Tamás, J. 2018. Wheat and maize yield forecasting for the Tisza river catchment using MODIS NDVI time series and reported crop statistics. *Computers and Electronics in Agriculture* 151 41-49.
- Sui, R. and Yan, H. 2017. Field study of variable rate irrigation management in humid climates. *Irrigation and Drainage*. 66: 327–339. DOI: 10.1002/ird.2111
- Tamás, J., Nagy, A. and Fehér, J. 2015. Agricultural biomass monitoring on watersheds based on remote sensed data, *Water Science and Technology* 72. 12. 2212-2220.

TOWARDS A SATELLITE-BASED DELINEATION AT THE TERRITORIAL SCALE IN HIGH YIELDING ENVIRONMENT TO SUPPORT THE MANAGEMENT OF NITROGEN

Lenoir A.¹, Dumont B.¹ & Vandoorne B.¹

¹*University of Liège, Junia, UMRT 1158 BioEcoAgro - Conduction, optimization and design of cropping systems meeting multi-criteria objectives, B-5030 Gembloux, Belgium*

Smart farming appears as a new opportunity to tackle European agriculture challenges. For decades, N fertilization methods endeavored to explicitly define features of soil supply and crop demand at the field scale. Poor nitrogen use efficiency (NUE) observed in crop production in western Europe proved the proposed methods to be unsuitable to accurately manage nitrogen (Zhang et al., 2015). An interesting method firstly developed by Blackmore (2000) and implemented by Basso et al. (2007) delineates management zones from spatial and temporal analysis of yield maps. In this method, fields are divided into high and stable yield zones, low and stable yield and unstable yielding zones. Each zone can be managed following specific approaches designed to maximize NUE. Evaluated on corn and soybean, the method has shown promising benefit to improve NUE compared to actual practices at the scale of USA (Basso et al. 2019). To the author's knowledge, such a program has not been conducted yet to develop nitrogen (N) management methods; its potential benefit must be demonstrated on winter wheat production in the European context where N management practices slightly differ. In the western European context, access to yield maps on a broad scale is constrained by yield monitor adoption (Lachia 2020). A body of literature has evaluated the relationship between yield and vegetation indices (VI) calculated from remote sensing devices (Diacono et al. 2013). Recently, Toscano et al. (2019) analyzed the relationship between yield distribution and in-field VI variations obtained through satellite images. Significant correlation has been found on wheat in different contexts, but no specific period had been identified to better correlate during the growing period. This result questions the possibility of delineating management zones applying Blackmore's methodology to vegetation indices sensed at specific periods.

To retrieve yield distribution in the present study and delineate management zones, different vegetation indices (VI) were calculated with Sentinel-2 data and tested through the period from stem elongation (Z30 on Zadock's scale) to late flowering (Z69). Only images with cloud cover lower than 30% were selected. Two fields (F1, F2) situated in northern France with respective surfaces of 10.9 ha and 6.3 ha have been specifically analyzed on three years of history, from 2016. Two other fields in the same area, for which data are only available in 2020, have also been studied (surfaces of 11.6 and 8.9 ha). Yield maps were cleaned beforehand according to the method proposed by Lyle et al. 2014. Blackmore's method of delineation applied to the fields only included wheat and barley as these two crops supposed a closer resulting interaction to pedoclimatic context than e.g., rapeseed or potatoes (Bjarne & Steffen, 2003). Besides the NDVI, different VI were calculated according to their robustness in high levels of biomass (MSR), their weak sensitivity to chlorophyll concentration variations or to soil disturbance (MCARI2, MTVI2) (Haboudane, 2004). The Spearman correlation between these indices and yield distribution has been calculated at each sensing date available during the above-mentioned period, each year. Correlation is considered significant when 95 % confidence interval excludes zero. To apply Blackmore's delineation method on indices maps, sensitivity of chosen dates has been evaluated through different scenarios. Scenarios 1 and 2 calculated management zones from images taken in homogeneous periods when correlations are among the highest. Scenario 3 uses, each year, the highest correlations even if sensing dates are not involved in the same period and is used to evaluate previous scenarios. Only dates with significant correlations were maintained. These scenarios were then compared to the initial yield map-based delineation.

The matching percentage between indices and yield maps of each zone was calculated to evaluate the accuracy of each sensing date scenario.

Delineation of management zones in fields F1 and F2 revealed very limited unstable zones, respectively 1.5% and 1% of field F1 and F2 areas. Instability over these fields is more a result of yield recording than real yield variations and is considered negligible. Zones corresponding to high and stable yield were observed on 53.4% and 47% of F1 and F2 areas whereas low and stable yield represent 45.1% and 52% of the fields. NDVI had slightly higher correlations (R: 0.38) than the other vegetation indices (R: 0.27) tested on each date and field, except MSR. However, NDVI values contrasted more through each period and were retained as VI candidate. Among the different sensing dates, 75% led to significant correlation to yield. Two periods seem to differentiate with higher correlations: 1st half of April and 2nd half of May with respective mean correlations of 0.34 and 0.43 calculated on the four fields and the period from 2016. Whatever the scenario considered, prediction potential of NDVI on management zone delineation reached 45%. This low value can be explained by different factors. Local yield variability is observed on every yield map, even after data cleaning. As prediction is calculated by pixel with high resolution, this variability limits its accuracy. Even if a trend between yield distribution and NDVI distribution exists, it would be interesting to investigate distribution of NDVI by ranges of yield values to explore sensitivity of the index.

- Basso, B., Bertocco, M., Sartori, L., Martin, E.C., 2007. Analyzing the effects of climate variability on spatial pattern of yield in a maize–wheat–soybean rotation. *European Journal of Agronomy* 26, 82–91. <https://doi.org/10.1016/j.eja.2006.08.008>
- Basso, B., Shuai, G., Zhang, J., Robertson, G.P., 2019. Yield stability analysis reveals sources of large-scale nitrogen loss from the US Midwest. *Science Reports* 9, 5774. <https://doi.org/10.1038/s41598-019-42271-1>
- Bjarne & Steffen, 2003. Intra-field yield variation over crops and years. *European Journal of Agronomy*. 19, 23 – 33. [https://doi.org/10.1016/S1161-0301\(02\)00016-3](https://doi.org/10.1016/S1161-0301(02)00016-3)
- Blackmore, S., 2000. The interpretation of trends from multiple yield maps. *Computers and Electronics in Agriculture* 26, 37–51. [https://doi.org/10.1016/S0168-1699\(99\)00075-7](https://doi.org/10.1016/S0168-1699(99)00075-7)
- Diacono, M., Rubino, P., Montemurro, F., 2013. Precision nitrogen management of wheat. A review. *Agronomic Sustainable Development* 33, 219–241. <https://doi.org/10.1007/s13593-012-0111-z>
- Haboudane, D., 2004. Hyperspectral vegetation indices and novel algorithms for predicting green LAI of crop canopies: Modeling and validation in the context of precision agriculture. *Remote Sensing of Environment* 90, 337–352. <https://doi.org/10.1016/j.rse.2003.12.013>
- Lachia, N., 2020. Usage des capteurs de rendement. Observatoire des usages de l’agriculture numérique. (Yield monitor adoption - Numeric agriculture custom observatory). http://agrotic.org/observatoire/wp-content/uploads/2020/04/infogra_Capteurs-de-rendement_-mai-2020.pdf (last accessed 29/04/21)
- Lyle, G., Bryan, B.A., Ostendorf, B., 2014. Post-processing methods to eliminate erroneous grain yield measurements: review and directions for future development. *Precision Agriculture* 15, 377–402. <https://doi.org/10.1007/s11119-013-9336-3>
- Toscano, P., Castrignanò, A., Di Gennaro, S.F., Vonella, A.V., Ventrella, D., Matese, A., 2019. A Precision Agriculture Approach for Durum Wheat Yield Assessment Using Remote Sensing Data and Yield Mapping. *Agronomy* 9, 437. <https://doi.org/10.3390/agronomy9080437>
- Zhang X., Davidson E., Mauzerall D., Searchinger T, Dumas P., Shen Y., 2015. Managing nitrogen for sustainable development. *Nature*, 15743. <http://doi:10.1038/nature15743>

WHY THE EVALUATION OF SPATIALIZED CROP MODELS NEEDS TO DIFFER FROM CURRENT APPROACHES TO MODEL EVALUATION?

Pasquel D.¹, Roux S.², Richetti J.³, Cammarano D.⁴, Tisseyre B.¹, Taylor J.A.¹

¹*ITAP, Univ. of Montpellier, Institut Agro Montpellier, INRAE, Montpellier, France*, ²*MISTEA, Univ. of Montpellier, Institut Agro Montpellier, INRAE, Montpellier, France*, ³*CSIRO Agriculture & Food, Floreat, WA, Australia*, ⁴*Department of Agronomy, Purdue University, West Lafayette, IN, USA*

Most existing crop models are “point-based models” (Heuvelink et al., 2010). Spatialization is the application of point-based models spatially across an area to apply these models to new scenarios without fundamentally changing the underlying model. Spatialization of crop models is of interest to the agricultural community as predictive crop modelling, particularly short to medium term predictions at field or subfield scales, is becoming an important part of modern site-specific management. The difference between a spatializing crop model and a spatial crop model is important. Spatialized models do not take into account neighbouring data or effects to compute a result at a point (or unit support) (Heuvelink et al., 2010). True spatial models do. Model evaluation refers to the question of knowing how close model predictions are to real observations, the aim is to ascertain the value of predictions computed by the models. This evaluation has to match with the proposed use of the model (Wallach et al., 2014). To evaluate if a predictive crop model is a good representation of variables it is supposed to simulate, a very common practice is to compare observed data versus simulated data (outputs). It can be in a qualitative way with a graph for instance or in a quantitative way by using some statistic that measure the distance between observed and simulated data (Wallach et al., 2014). Lots of these statistics are used in the literature, the most common are : coefficient of determination (R^2), Bias, Mean Square Error (MSE), Root Mean Square Error (RMSE), Nash-Sutcliffe Efficiency (NSE) and Willmott index of agreement (D-index). All of these statistics are aspatial. In the case where they are applied to a spatialized (or spatial) model, there are no spatial characteristics of the model predictions taken into account. Such statistic utilization may affect the evaluation of spatialized crop models, particularly when the spatialization of the models is usually dependent on the availability of spatially autocorrelated environmental inputs (Zhao et al., 2016). Incorporating these data into the model may mean that errors (i.e. difference between observed and simulated data) are not independent. Therefore, spatial autocorrelation in the inputs or outputs can violate assumptions of many statistical metrics.

To illustrate the issue and the need for new approaches to spatialized crop model evaluation, a simple case study is presented. The aim of the case study is to demonstrate the limitation of aspatial statistics that have been widely used for the evaluation of spatialized crop models in the recent literature. In this case, the RMSE is used as the example statistic as this is the statistic most commonly used in studies. In the example, the intent is to define management zones (MZ) within a vineyard for the purpose of precision viticulture. The predicted variable that is used to define these MZs is predawn leaf water potential (PLWP). The purpose of this example is to show that with different theoretical spatial models of PLWP, the outcome of clustering based on the PLWP predictions can be variable and independent of the RMSE.

The simulated example is built on real observed data of PLWPs on a 1.2 ha Shiraz vineyard in 2003. This vineyard is located in Pech Rouge (INRAE Gruissan, 43°08'47" N, 03°07'19" E). To simulate the output from various potential spatialized crop models, a series of noise models were constructed, all following a normal distribution with a fixed mean (0) and variance (0.2) but with various levels of spatial structure within the noise models. Two of the noise distributions were dependent on the observed PLWP (some spatial structure), while the third distribution was random (i.e. independent from observed PLWP). Maps of the original data and

the simulated spatialized models are in Table 1. The original PLWP data were made into MZs based on tertile analysis and the threshold values from this analysis used to create the MZs in the simulate PLWP maps. The agreement between the MZ maps was determined using the Kappa statistic.

RMSE is calculated from the simulated PLWP (i.e. sum of observed PLWP and attributed noise) and the observed PLWP, and should identify which simulation is better from the others. However, because the simulated noise models have the same distribution (but different spatial structure) the RMSE in these cases was identical (Table 1). Therefore, the conclusion is that all three models were equally good, and the defined MZs should be equally good.

Table 1: Management Zones (MZ) based on a classification of 3 classes using the observed and simulated Predawn Leaf Water Potential (PLWP) models showing the RMSE and Cohen’s Kappa value associated with the simulated models.

	Observed PLWP	Simulated PLWP		
	Real Data	Model 1	Model 2	Model 3
MZ				
RMSE		0.16	0.16	0.16
Cohen’s Kappa		0.64	0.05	0.31

The resulting MZ maps for the three models do not support this, nor do the Kappa values. Even though the RMSE is constant, the Model 1 spatial pattern was much closer to the original data (higher Kappa value) than Model 2 or 3. Model 2 had the least similar spatial pattern to the observed data (lowest Kappa value). Thus, even though the RMSE was the same on these three simulations, the derived MZs were significantly different between simulations. Selecting the best MZ (i.e. from the best spatialized model) cannot be decided with only the RMSE.

If predictive crop modelling using spatialized crop models is to become a common aspect of Precision Agriculture then new methods or statistical metrics that take into account the spatial characteristics of the data and models will be needed to evaluate these crop models.

Heuvelink, G.B.M., Brus, D.J., Reinds, G., 2010. Accounting for spatial sampling effects in regional uncertainty propagation analysis. In : proceedings of the 9th International Symposium on Spatial Accuracy Assessment in Natural Resources and Environmental Sciences, Leicester, UK, pp. 85–88.

Wallach, D., Makowski, D., Jones, J.W., Brun, F., 2014. Working with dynamic crop models - Methods, tools and examples for agriculture and environment, 2nd ed. Elsevier.

Zhao, G., Hoffmann, H., Yeluripati, J., Xenia, S., Nendel, C., Coucheney, et al., 2016. Evaluating the precision of eight spatial sampling schemes in estimating regional means of simulated yield for two crops. *Environmental Modelling & Software* **80** 100–112.

AGRO IOT PLATFORMS AND SENSORS IN CROP PRODUCTION

Ambrus B., Nyéki A., Teschner G. , Neményi M. , Milics G., Kovács A. J.
Széchenyi István University, Faculty of Agricultural and Food Sciences, Department of Biosystems and Food Engineering, Mosonmagyaróvár, Vár 4., Hungary
ambrus.balint@sze.hu

This study presents the objectives and the framework of Agronomic - Internet of Things system in Mosonmagyaróvár (M-AIoT), taking place at Széchenyi István University Faculty of Agricultural and Food Sciences, such complexity is the first time in Hungary. The core part of this activity is automating data collection, extended with remotely-sensed parameters of crops, resulting in real-time data from the devices with programmable time sequences. The structure of IoT is based on three layers: the sensing layer, the data transfer layer and the application layer. The M-AIoT system is designed to collect data from a crop field and also from the surrounding natural areas. In this case, the relationship between natural ecology and agro-ecology can be profoundly studied. Complementing M-IoT data with data from UGVs (mobile robots), UAVs and satellites, the requirements for sustainable (both environmentally friendly and profitable) precision farming can be fulfilled.

In this study, the different base sets of sensor that were installed to collect data from soil, atmosphere, plant and the environment, sampling every 16 minutes were demonstrated. The devices were installed in a 6 ha corn and a 15 ha wheat fields (Fig. 1.). These devices have been installed in the crop, on different types of soil (sandy loam, loam, silt loam) in the year 2019 and 2020 (Nyéki et al, 2020).



Figure 1: Position of the sensors in the research fields.

The M-AIoT system integrates commercially available devices such as Libelium (URL¹), Boreas (URL²), and Campbell Scientific (URL³) sensors and self-developed data collection devices.

The monitoring parameters are: soil electrical conductivity, soil oxygen content, soil temperature and moisture at different depths, leaf wetness, air temperature, humidity and pressure, and ground water properties. Three sensors have been installed in an artificial water pit to detect the pH and the nitrite and nitrate content of the ground water. The system also includes a complex meteorological station. The sensor system also collects and transmit parameters from

the crop micro-climate (i.e.: global radiation, rain gauge, wind speed and direction). All the measurement units are powered with efficient solar panels, supplying energy even in cloudy and short daylight (wintertime) conditions.

A robotic measuring unit was developed in order to collect further data not collected by the sensor system. The applicability of mobile data loggers and installed sensor station were examined in this project. The power supply, the failures of communication and the data loss are monitored on a self-developed web-based interface. The web-based interface was designed to integrate the incoming data from different sensors using dissimilar communication protocols (LoRaWAN, GSM). Majority of the online data transmission (90%) is based on LoRaWAN communication protocol. The server development was implemented in .NET language. MS SQL database was used to store the data collected by the various sensors.

The aim of the IoT-based web interface development was to create a farmer-centric system that visually interprets the data, enhancing the useful information for the farmers.

Furthermore, this information is accessible from any platform (i.e. PC or smartphone) allowing the research team to automatically obtain data and make decisions in a faster and more efficient way. Therefore, a website was developed that already supports useful tools that were developed in an angular framework. The web interface is designed to handle the different measuring stations from crop fields uniformly. This web-based system can provide a comparative and valuable analysis with the experiences and conclusions of the different sensors accuracy and usability in the field. Based on experience with the system, the farm advisory extension can be supported. The analysis can help the farmers to make better decisions related to field management (e.g. optimal time for sowing, optimum nitrogen fertilizer amount and irrigation recommendation). Based on the development and measurement results of the project so far, further development of the system is needed. During the operation, the reliability of data transmission errors of the sensors, the discharge of the battery, the displacement of the soil sensors and wildlife damage became problems. According to experience, the functionality of the complex system has to be improved by advancing analytical features. Furthermore, it is intended to implement effective prediction of sensors database using artificial intelligence. Therefore, farmers will be able to manage their field more efficiently.

ACKNOWLEDGEMENTS

This project is financed by “Thematic Area Excellence Program” (TUDFO/51757/2019-ITM) and GINOP-2.3.4-15-2016-00003 (FIEK project).

REFERENCES

Nyéki, A., Teschner, G., Ambrus, B., Neményi, M., Kovács, A., J. 2020. Architecting farmer-centric internet of things for precision crop production. *Hungarian Agricultural Engineering* **38** 71-78.

(URL¹): <https://www.libelium.com/libeliumworld/success-stories/hungarys-first-field-monitoring-lab-relies-on-libeliums-iot-technology/>

(URL²): <http://www.boreas.hu/index.php?src=&lang=eng>

(URL³): <https://www.campbellsci.com/>

DEVELOPMENT OF A LOW-COST PORTABLE PAR DEVICE FOR CROP MANAGEMENT

Coffin A.¹, Bonnefoy-Claudet C.², Jansen A.² and Chassigne M.², Gée C.¹

¹Agroécologie, AgroSup Dijon, INRAE, Univ. Bourgogne, Univ. Bourgogne Franche-Comté, F-21000 Dijon, France. ² AgroSup Dijon, 26 boulevard Docteur Petitjean, 21000 Dijon, France.

In the context of climate change and innovative agroecological practices, it is essential to have precise monitoring of crop growth to ensure rapid action in case of problems. Plant growth depends on the biomass accumulated by photosynthesis that requires as energy source, photosynthetically active radiation (PAR). This variable is essential to study plant phenology and for ecophysiological models allowing prediction of biomass with daily determination of dry matter accumulated (STICS: Brisson et al., 2003; APSIM: Keating et al., 2003; AZODYN: Jeuffroy and Recous, 1999). Thus, because of field microclimate, PAR sensors need to be placed close to the field. However, commercial measuring instruments consist of a data logger and one or more sensors and are too expensive. In addition, a PAR sensor is rarely installed on automatic weather stations. The objective of this study is to propose an innovative device development, a low-cost miniaturized solution which is robust and energy autonomous and that can easily be moved from one field to another.

An engineering solution to design, implement and calibrate a PAR measurement device (SOLEM PAR/LE) combined with an open-source electronic platform (Arduino) is presented. The device is named PARADe (PAR Acquisition Device). The PAR sensor was calibrated by comparison with a calibrated sensor (PQS1 PAR Quantum Sensor, Kipp & Zonen) and an industry standard data-logger (CR1000 Campbell Scientific).

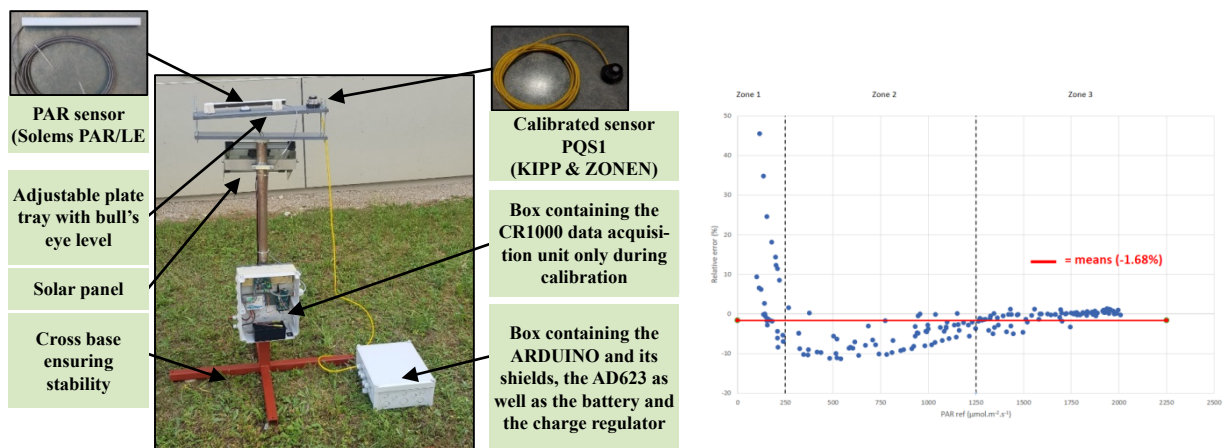


Figure 1: Left: Portable PAR device, Right: Relative error as a function of actual PAR.

The ARDUINO card records the PAR sensor voltage through an AD623 amplification (rail-to-rail amplifier) every five seconds in its internal memory. After 60 values (i.e. 5 minutes), it calculates the average of the voltage values and writes it to the microSD card. The average of the 60 measurements is recorded every 5 minutes to reduce the variability from the ARDUINO and the sunshine conditions. To make the calibration curve relating the output voltage of the PARADe acquisition chain to the radiation, it is necessary to place the calibrated sensor close to the sensor to be calibrated (Figure 1, left). To test good repeatability of the device, measurements were taken at different days or times of the day, in different places, in the shade, and in the sun. To verify the accuracy of PARADe measurements, a relative error (RE) profile was carried out.

This profile is a graph showing RE (defined by Eq. 1) as a function of the actual PAR.

$$\text{Relative error} = ((\text{PAR}_{\text{device}} - \text{PAR}_{\text{ref}}) / \text{PAR}_{\text{ref}}) * 100 \quad (1)$$

With two different PAR values: the amount of PAR_{ref} which is determined using the calibrated sensor connected to the CR1000 data logger and that of the $\text{PAR}_{\text{device}}$ obtained by the calibration equation of PARADe.

The graph in Figure 1 (right) represents this relative error profile of the PARADe device. On average, the portable device with the ARDUINO card has a relative error of -1.68%. In this figure, the strong errors observed at low PAR values are ultimately inherent due to the shape of the sensor and do not defeat the acquisition chain. Following Standard ISO 9847, it emerges that in practice the radiation measurements for which the solar altitude angle is less than 20° (at sunrise sun and sunset) are excluded. It is due to the poor quality of response to the radiation of this type of rectilinear sensor (Standard ISO 9847: 1992). The calibration curve can therefore be kept.

Compared to other portable devices available (Barnard et al., 2014), the PARADe device appears to be as effective or even superior for high PAR radiation. These results make its use operational. These PAR measurements can then be used as input parameters for ecophysiological models. In perspective, a smartphone, a digital tablet or a laptop could be the interface with the device via a Bluetooth or Wi-Fi connection.

REFERENCES

- Barnard, H. R., Findley, M. C., Csavina, J. (2014) PARduino: A Simple and Inexpensive Device for Logging Photosynthetically Active Radiation. *Tree Physiology* 34 640-645. <https://doi.org/10.1093/treephys/tpu044>
- Brisson, N., Gary, C., Justes, E., Roche, R., Mary, B., Ripoche, D., et al. (2003). An overview of the crop model STICS. *European Journal of Agronomy* 18 309-332.
- Keating, B. A., Carberry, P. S., Hammer, G. L., Probert, M.E., Robertson, M. J., Holzworth, D., et al. (2003). An overview of APSIM, a model designed for farming systems simulation. *European Journal of Agronomy* 18 267-288.
- Jeuffroy, M. H., Recous, S. (1999). Azodyn: a simple model simulating the date of nitrogen deficiency for decision support in wheat fertilization. *European Journal of Agronomy* **10** 129–144.
- SOLEMS S.A. 2011. https://www.solems.com/wp-content/uploads/PAR_LE_mode_d_emploi_fr.pdf.

OPPORTUNITIES FOR MORE PRECISE WEED MANAGEMENT IN FIELDS OF LOWLAND RICE IN SOUTH-EASTERN NIGERIA.

Ukwoma-Eke, O., Murdoch, A. J.

School of Agriculture, Policy and Development, University of Reading, Reading, U.K.

Rice is the most important food in Nigeria, but hunger is still widespread. Weed infestations are a major constraint to raising rice yields. Farmers struggle to rescue their harvest from some of the world's worst weeds using hand weeding and the uniform application of herbicides across whole fields. If the weeds accumulate in patches, then precision agriculture could be implemented as site-specific weed management (SSWM). In the absence of technology, this study explores the introduction of SSWM by adapting traditional knowledge and practices to enable farmers to target interventions more precisely to weed patches.

The study area was Ayamelum Local Government Area of Anambra State, SE Nigeria. The major crop in the area is rain-fed rice, technology is low, most fields are less than a hectare and are cropped once in a season. Questionnaires were administered to 281 lowland rice farmers in the study area. The responses from the questionnaire were summarized using IBM SPSS Statistics 24.

In addition, two lowland rice fields were sampled as an independent verification of respondents' claims. These fields were chosen randomly from among the fields belonging to farmers who had indicated that the weeds in their fields were spatially-variably distributed. Within each field, flooding depth and populations of two weeds, *Nymphaea maculata* Schumacher & Thonn and *Echinochloa* spp., were assessed. An 8 m regular grid with some nested samples at 2 m intervals provided 90 96 sampling sites per field, in which weeds were counted a 63.2 cm square quadrat. Variograms were computed using Matheron's method of moments (Mahmood & Murdoch, 2017). Flooding depth was mapped by ordinary kriging, but the inverse distance weighting method (Oliver & Webster, 2014) was used for weed mapping since both weeds were absent in up to 60% of the quadrats. All maps were prepared with ArcGIS software edition 10.4. Correlations and experimental variograms were computed using GenStat 18th edition.

In describing the weed distribution in their fields, 71% of the respondents indicated that the weeds were spatially-variably distributed and 69% of these respondents associated the patchiness of weeds with differences in flooding depth. Most respondents stated that they observed higher densities of *N. maculata* in flooded portions of their fields while *Echinochloa* spp. often accumulated in the drier parts. Visually, the maps of weed density and flooding depths in two fields appear to corroborate these claims (Figure 1). The variograms confirmed that there was significant spatially-correlated variation of the weeds and flooding in both fields even though the fields were <1 ha. The variation in the flooding depth reached a maximum (sill variance) at 50 and 170 m in fields one and two, respectively (compare Figure 1). Although some parts of each field were dry at the time of sampling, about 50% of both fields was flooded to a depth of >5 cm. The maximum measured flooding depths were 25.6 and 30 cm in fields one and two, respectively. The highest densities of *N. maculata*, i.e., 11 and 31 plants m⁻² in fields one and two respectively, were observed at flooding depths of 20-30 cm. This species only occurred in areas with >6 cm flooding depth and correlated positively with increasing flooding depth ($R = + 0.6$ to $+ 0.7$) (Figure 1). By contrast, *Echinochloa* spp. appeared to aggregate in drier parts of both fields, and there was a negative correlation of ($R = - 0.4$) between *Echinochloa* spp. populations and increasing flooding

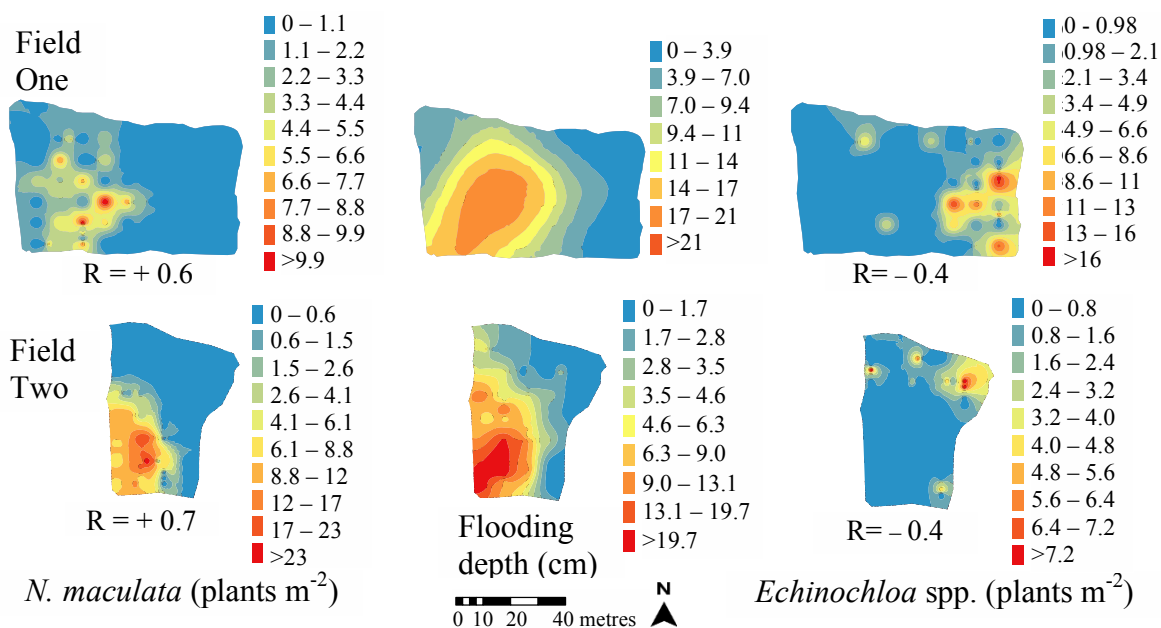


Figure 1: Maps of the distribution of *N. maculata* (left), *Echinochloa* spp. (right) and flooding depth (centre) across two lowland rice fields in SE Nigeria.

R refers to the Pearson's correlation coefficient between flooding depth and weed population.

Note that the colour scale differs on each map.

depth in both fields (Figure 1). The highest population of *Echinochloa* spp., 19 plants m⁻² in field one, occurred in a part of the field with <3 cm of flooding.

In field two, the greatest density of *Echinochloa* spp. was 8 plants m⁻² and this was observed in a completely dry part of the field. The maps of both fields show a quick decline in *Echinochloa* spp. populations as the flooding depth exceeds 6 cm (Figure 1).

The farmers were clearly aware that flooding was influencing the weed distribution in their fields. Though the fields are small, the data indicates that the weeds in individual fields could be spatially variably distributed, perhaps especially where the fields were not level and the depth and duration of flooding varies. More precise interventions might, therefore, achieve satisfactory weed control, reduce herbicide and labour costs and minimise any adverse environmental impacts of herbicide use. Interestingly, some farmers were adopting SSWM immediately following the study. Many farmers, who had participated in the survey, subsequently applied different types of herbicides in different parts of their fields based on the weed species and levels of infestation they observed. Others changed their negotiations with the labourers for hand weeding, from the traditional whole-field basis to a weed-patch basis.

In future, farmers could demarcate weed management zones based on flooding depth and expected weed infestations. Zones could also be banded to flood to desired levels. SSWM in this way would allow different doses or types of herbicide and varying hand weeding schedules.

Mahmood, S. A. and Murdoch, A. J. 2017. Within-field variations in sugar beet yield and quality and their correlation with environmental variables in the East of England. *European Journal of Agronomy* **89** 75-87.

Oliver, M. and Webster, R. 2014. A tutorial guide to geostatistics: Computing and modelling variograms and kriging. *Catena* **113** 56-69.

ENCOURAGING TECHNOLOGY TAKE-OFF WITH FARMER CHAMPIONS AND STUDENT AMBASSADORS

G. Rose¹, A.J. Murdoch¹, D.S. Paraforos², T. Pavlenko², J. Draper³, L.M. Battaglini⁴, P. Cornale⁴, M. Renna⁵, N. Scollan⁶, I. Marshall⁶, R. Negrini⁷, M. Favoro⁷ and I. Pascarella⁷

¹University of Reading, School of Agriculture, Policy and Development, Earley Gate, PO Box 237, RG6 6EU, UK, ²Hohenheim University, Agricultural Engineering, Garbenstrasse 9, 70599 Stuttgart, Germany, ³Anglo Beef Processors UK (ABP UK), 6290 Bishops Court, Birmingham Business Park, West Midlands B37 7YB, UK, ^{4,5}Università degli Studi di Torino, ⁽⁴⁾DISAFA and ⁽⁵⁾DSV, largo Paolo Braccini, 2, 10095 Grugliasco Turin, Italy, ⁶Queen's University of Belfast, Biological Sciences, Lisburn Road, Belfast BT9 7BL, UK, ⁷Associazione Italiana Allevatori - AIA, Via G. Tomassetti, 9, 00161 - Roma, Italy

Focus on Farmers was funded by EIT Food as three projects, one in each of 2018, 2019 and 2020. All three projects engaged farmers and encouraged technology adoption by arable and livestock farmers in the UK, Italy and Germany. Engaging primary producers and the students were key elements in introducing new technologies and promoting their adoption. Sector-specific engagement activities were key to success and ensured the activities were tailored to the audience whether dairy farmers producing milk for Italian PDO cheese producers, dealers of John Deere machinery in Germany or beef farmers in the UK. Student ambassadors and farmer champions, therefore, played key roles in the project. The students brought new knowledge and skills with lots of ideas and enthusiasm. Farmer champions and technology ambassadors help to nudge 'laggards' towards technology adoption. By their example, other farmers could see the benefits of technology adoption and learn from others. Farmers gained confidence through visiting their peers and seeing and discussing how technology was implemented. In 2020 with Covid-19, virtual farm walks and webinars with farmer champions and researchers were highly effective way of exposing, for examples, beef farmers to precision approaches such as rotational paddock grazing. Farmers thus learned from the success of others supported by specialists who ensure the science behind recommendations. A Farmer Technology Framework was therefore proposed in 2019 and has been implemented in 2020.

In this framework, the industry partners identify suitable farmer champions (also technology champions). These champions would ideally be early-adopters of precision agricultural technology and demonstrate a passion for adapting technology with a history of successful adoption. They also demonstrated excellent interpersonal skills and were committed to communicating the benefits of technology to their peers. The industry partners and champions identified engagement opportunities, which are likely to be dependent on industry. For example, ABP organised a farm visit and, with Covid-19, a series of webinars for beef farmers in Northern Ireland and England in association with Queen's University and the University of Reading. AIA in Italy delivered a report to 12000 dairy farmers with whom they have links. The industry partners advertised and helped to recruit farmers to attend the engagement activities. The champions, in collaboration with the industry partner, hosted the event, focusing on highlighting the use of technology and the benefits to the farming enterprise of the chosen technology.

In order to encourage greater adoption, a farmer-to-farmer approach with farmer champions was important to overcome reluctance by farmers to adopt innovation on their farms, especially when related to sensitive topics such as animal welfare. Moreover, to foster laggard-farmers to adopt innovations, tools and documents need to be customized to take account of variables such as herd size and genetic potential, existing farm automation and the education level of farmers.



Figure 1: Examples of farmer and student engagement to encourage precision technology adoption

Farmers were engaged with farmer champions and student ambassadors to appropriate technologies in a variety of events (e.g. Figure 1). Despite a very modest budget, the project reached 6,252 farmers and students in a range of events in 2019. The live webinars in 2020 reached a total of 2,072 farmers with an additional 1,503 viewers accessing the YouTube recording. In addition, the Facebook reach totalled 33,129.

Technology helps address major issues from improving productivity on farm through to reducing greenhouse gas emissions from farming systems to improving animal welfare and reducing fraud. To advance this area further, it is essential to have multi-disciplinary teams working together from producers, processors to consumers, supported by technology providers/ developers, agronomists and scientists. It was also evident that there is much work and a huge appetite among farmers for education in uses of outputs from digital technologies, to help improve their businesses. There are also issues associated with lack of robust broadband/internet access in rural areas to help advance application of the technology. However, one benefit of Covid-19 has been the very successful use of webinars to reach large numbers of farmers.

ACKNOWLEDGEMENTS

This EIT Food activity has received funding from the European Institute of Innovation and Technology (EIT), funded by the European Union, under the EU Horizon2020 Framework Programme for Research and Innovation.

We are also grateful to the farmers and students who participated in the activities in Italy, Germany and the UK

NUDGING ARABLE FARMERS TOWARDS GREATER ADOPTION OF PRECISION AGRICULTURE

Antognelli, S.¹, Murdoch, A.², Guidotti, D.¹, Ranieri, E.¹, Ahrholz, T.³, Tranter, R.², Engel, T.³, Mahmood, S.², Paraforos, D.S.⁴, Todman, L.²

¹*Agricolus srl, via Settevalli, 320, 06129 Perugia (Italy)*, ²*School of Agriculture, Policy and Development, The University of Reading, Earley Gate, PO Box 237, Reading RG6 6AR, U.K.*, ³*John Deere GmbH & Co. KG, European Technology Innovation Center, Straßburger Allee 3, 67657 Kaiserslautern, Germany*, ⁴*University of Hohenheim, Institute of Agricultural Engineering, Technology in Crop Production (440d), Garbenstr. 9, D-70599, Stuttgart, Germany*

Farmers increasingly generate large amounts of data for their fields but often the way to use the data is unclear. While data can be viewed on its own, the LINKDAPA software platform aims to create innovative predictive synergies by linking historical and current data for winter wheat crops. In this way, farmers would have the instruments to obtain the most of the informative potential from their data. LINKDAPA (Linking multi-source Data for Adoption of Precision Agriculture) is being co-funded by the EU-supported EIT Food. The project is nudging farmers towards greater adoption of precision agriculture first by involving them in developing novel ways of looking at their “big” data and in developing the platform and secondly, by emphasising financial sustainability – predicting the probability that a higher profit could be achieved by adopting PA.

Eight key farmers in Italy, Germany and the UK identified aspects of PA of greatest interest and indicated the clarity, usefulness and attractiveness of a ‘mock-up’ platform. The mock-up platform included different sections with different features. The first section is the entry page, which reports synthetic information about each field status, and make different information of different fields easy to compare. The entry page includes a table, in which each row is dedicated to a field. The columns report different synthetic information, including the crop and variety planted on the fields, the average NDVI from Sentinel 2 of the last available date, the average yield (from yield map uploaded in the system), the average protein content (from protein maps uploaded in the system), and the list of available maps for each field.

Field name	Varieties	Last avg yield	Last average proteins	Last ndvi	Available maps
CP 13	N/A	N/A	N/A	N/A	<ul style="list-style-type: none"> ✗ Yield map ✗ Protein map ✗ Prescription map
CP 19	N/A	7.63 t/ha Jul 1, 2020	14.65 % Jul 1, 2020	N/A	<ul style="list-style-type: none"> ✓ Yield map ✓ Protein map ✗ Prescription map
CP 23b	N/A	N/A	N/A	N/A	<ul style="list-style-type: none"> ✗ Yield map ✗ Protein map ✗ Prescription map
CP 26	N/A	9.4 t/ha Jul 1, 2020	11.47 % Jul 1, 2020	N/A	<ul style="list-style-type: none"> ✓ Yield map ✓ Protein map ✗ Prescription map
CP 29	N/A	8.72 t/ha Jul 1, 2020	N/A	N/A	<ul style="list-style-type: none"> ✓ Yield map ✗ Protein map ✗ Prescription map

Field name	Varieties	Last avg yield	Last average proteins	Last ndvi	Available maps
CP 1a	N/A	N/A	N/A	0.74 Nov 29, 2020	<ul style="list-style-type: none"> ✗ Yield map ✗ Protein map ✗ Prescription map

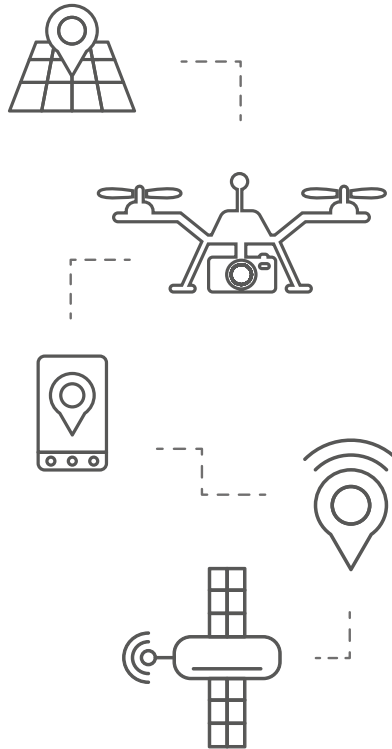
Figure 1: example of the summary information for each cereal field

The second section is the detail page of each single field, that reports more specific information. The user can navigate the map of the winter cereals fields of the farm, visualizing crop or variety, yield maps, protein maps, and the last available NDVI. This section also allows the user to upload and visualize yield or protein maps collected on field, to visualize the yield and protein prediction, and to create his own prescription map for variable rate fertilizer applications for the selected field. Prescription maps meet the need to customize fertilizer rates for each area of the field on a spatially-variable basis.

Prescription maps support the optimization of the fertilizer dose, prescribing the predicted optimum variable rate fertilizer amount in each part of the field.

In order of importance, farmers expressed their interest in: 1. Prescription map for variable rate applications (VRA) of N in spring 2. A means of linking all historical farm data for single field 3. View recent satellite vegetation map 4. Prescription map for VRA of seed 5. Maps of each field during the growing season predicting a) wheat yield, moisture, and protein; b) the probability that adopting a PA option would increase revenue and profit compared to a uniform treatment; c) the probability that grain yield, moisture and protein would exceed farmer-specified targets. Novel field zoning options were also discussed with the farmers. These options includes: 'don't apply many inputs in zone B as it won't yield well; spend more in zone A, which is likely to yield >10 t/ha'. Zonal harvesting have also been presented as an alternative opportunity, as it become possible in the last years, thanks to new machineries and technologies. For example, 'zone D is likely to yield high protein grain but zone C is not'. These discussions with farmers were carried on to identify their potential interest on them, and to provide ideas for a data centric, new approach to cereal farming.

published by Hungarian Society of Precision Agriculture
address: 1149 Budapest Angol Street 34.
phone number: +00 36 70 364 5518
e-mail: elnok@preciziosklub.hu
web page: www.preciziosklub.hu
contact person: Anna Dvorszky
editors: John V. Stafford, Dr. Gábor Milics
ISBN 978-615-01-2017-1



The Hungarian organisers are pleased to welcome the ECPA conference to Budapest, even in this very difficult pandemic situation. The conference is organised in hybrid form, the presenters and participants can join the event online or in person. With this solution we can reach 400 participants.

The aim of the Ministry of Agriculture is to lead the Hungarian farmers into the digitized era of agriculture. A scientific conference is always the best way to promote development. The conference is focusing on the new scientific results and adoption of innovative precision agriculture technologies and solutions.

Hungarian Society of Precision Agriculture
(Magyarországi Precíziós Gazdálkodási Egyesület)
1149 Budapest Angol Street 34.

For more information, please email: ecpa2021@ecpa2021.hu
Website: <https://www.ecpa2021.hu/>